Late Oligocene–early Miocene submarine volcanism and deep-marine sedimentation in an extensional basin of southern Chile: Implications for the tectonic development of the North Patagonian Andes

Alfonso Encinas[1,†], Andrés Folguera[2], Verónica Oliveros[1], Lizet De Girolamo Del Mauro[1], Francisca Tapia[1], Ricardo Riffo[1], Francisco Hervé[3,4], Kenneth L. Finger[5], Victor A. Valencia[6], Guido Gianni[2], and Orlando Álvarez[7,8]

[1]*Departamento de Ciencias de la Tierra, Facultad de Ciencias Químicas, Universidad de Concepción, Concepción 4030000, Chile*

[2]*Instituto de Estudios Andinos "Don Pablo Groeber," Departamento de Ciencias Geológicas, Facultad de Ciencias Exactas y Naturales, Universidad de Buenos Aires–CONICET, Buenos Aires C1428EHA, Argentina*

[3]*Departamento de Geología, Facultad de Ciencias Físicas y Matemáticas, Universidad de Chile, Santiago 6511228, Chile*

[4]*Carrera de Geologia, Universidad Andres Bello, Salvador Sanfuentes 2357, Santiago 837-0211, Chile*

[5]*University of California Museum of Paleontology, Berkeley, California 94720, USA*

[6]*School of the Environment, Washington State University, Pullman,Washington 99164, USA*

[7]*Instituto Geofísico Sismológico "Ing. Fernando Volponi", Facultad de Ciencias Exactas, Físicas y Naturales, Universidad de San Juan, San Juan 5400, Argentina*

[8]*Consejo Nacional de Investigaciones Científicas y Técnicas, CONICET, Buenos Aires C1033AAJ, Argentina*

ABSTRACT

The Chilean margin has been used as the model of an ocean-continent convergent system dominated by compression and active mountain building as a consequence of the strong mechanical coupling between the upper and the lower plates. The Andean Cordillera, however, shows evidence of alternating phases of compressional and extensional deformation. Volcano-sedimentary marine strata in the Aysén region of southern Chile contribute to an understanding of the causes of extensional tectonics and crustal thinning that occurred in the Andean orogeny because these deposits constitute the only reliable record of submarine suprasubduction volcanism during the Cenozoic in southern South America. In order to discern the age and tectono-sedimentary setting of these strata, referred to as the Traiguén Formation, we integrated sedimentology, ichnology, petrography, geochemistry, structural geology, foraminiferal micropaleontology, and U-Pb geochronology. Our results indicate that the Traiguén Formation was deposited in a deep-marine extensional basin during the late Oligocene–earliest Miocene. The geochemistry and petrography of the pillow basalts suggest that they formed in a convergent margin on a thinned crust rather than at an oceanic spreading center. We attribute the origin of the Traiguén Basin to a transient period of slab rollback and vigorous asthenospheric wedge circulation that was caused by an increase in trench-normal convergence rate at ca. 26–28 Ma and that resulted in a regional event of extension and widespread volcanism.

INTRODUCTION

The East Pacific or Chilean margin is the archetypal example of an ocean-continent convergent system (e.g., Dewey and Bird, 1970; Charrier et al., 2002). Subduction along this margin has been taking place continuously at least since the Early Jurassic (Mpodozis and Ramos, 1990). A distinctive feature of the Chilean margin is the Andean Cordillera, the longest and highest active mountain chain in a subduction setting, which developed as a consequence of crustal shortening and magmatic addition (Jordan et al., 1983; Charrier et al., 2002).

The Chilean margin differs markedly from the West Pacific margin, which is characterized by a series of intraoceanic arcs and associated extensional marginal basins usually floored by mafic crust (Bartholomew and Tarney, 1984; Mpodozis and Ramos, 1990). Uyeda and Kanamori (1979) related the differences between both margins to the relatively young and buoyant oceanic crust that generates strong mechanical coupling between the upper and the lower plates and characterizes the "Chilean subduction mode." In contrast, the "Marianas subduction mode" is typified by weak coupling and extension resulting from subduction of old oceanic crust.

The Chilean margin has not been in a permanent state of compression during its long history (e.g., Mpodozis and Ramos, 1990). After a rifting event in the Triassic, subduction was reestablished in the Jurassic under extensional conditions (Mpodozis and Ramos, 1990). As a consequence, a series of interconnected backarc basins developed east of the new volcanic arc and were filled with marine and continental sedimentary strata (Mpodozis and Ramos, 1990; Mpodozis and Cornejo, 2012). By the early Late Cretaceous, a shift to a contractional tectonic regime resulted from the accelerated westward drift of South America in response to the final opening of the South Atlantic Ocean (Russo and Silver, 1996; Mpodozis and Cornejo, 2012). The backarc basins that had developed in the previous extensional regime were tectonically inverted, and the Andean Cordillera and its associated foreland basins started to develop (Mpodozis and Ramos, 1990).

The archetypal contractional "Chilean subduction mode" described by Uyeda and Kanamori (1979) seems to have predominated during the Late Cretaceous–Holocene interval, whereas the evolution of the Chilean margin during the Jurassic–Early Cretaceous would have resembled the "Marianas subduction mode" (Mpodozis and Ramos, 1990). However, geologic evidence indicates that the Andean margin has not been in a continuous state of compression since the Late Cretaceous, as pulses of major tectonic short-

[†]aencinas@udec.cl

doi:10.1130/B31303.1; 9 figures; Data Repository item 2015373.

ening have alternated with intervals characterized by moderate shortening or extension (e.g., Mpodozis and Ramos, 1990; Martinod et al., 2010). In addition, despite rather uniform convergence conditions along the Chilean margin for the same periods of time, the tectonic evolution of the Andean Cordillera shows remarkable latitudinal differences. Throughout most of the Cenozoic, the Andes of southern Peru and northern Chile (~15°S–27°S) have been subjected to ongoing compression (e.g., Oncken et al., 2006, and references therein), while the Andes of central and southern Chile (~33°S–46°S) have had alternating episodes of compressional and extensional tectonics (e.g., Jordan et al., 2001; Charrier et al., 2002; Orts et al., 2012; García Morabito and Ramos, 2012). The causes of variations in the tectonic regime both in time and space during Andean history are still not well understood and have been ascribed to several different causes, including changes in the convergence rate between the oceanic and continental plates (e.g., Pardo-Casas and Molnar, 1987), variations in the absolute westward motion of South America (e.g., Silver et al., 1998), changes in interplate coupling (Lamb and Davis, 2003; Yáñez and Cembrano, 2004), and modifications of the dip angle of the subducting slab (Jordan et al., 1983; Martinod et al., 2010).

The volcano-sedimentary marine deposits in the Aysén region of southern Chile (~45°S; Fig. 1) are pertinent to our quest to better understand what caused the alternating intervals of compression and extension that characterize the tectonic evolution of some segments of the Andes during the Cenozoic. These strata crop out in the present forearc of the cited region and constitute a succession of basaltic pillow lavas interbedded with marine sandstones and siltstones ascribed to the Traiguén Formation (Espinoza and Fuenzalida, 1971; Hervé et al., 1995; Silva, 2003). This unit was originally thought to be Early Cretaceous (Fuenzalida and Etchart, 1975), but subsequent studies favor the Cenozoic, although a refined age has remained elusive because this formation has been ascribed to the Miocene (Céspedes, 1975), late Oligocene (Hervé et al., 2001), and Eocene–middle Miocene (Silva et al., 2003). The origin of the Traiguén Basin is also debated, having been attributed to extensional tectonics (Bartholomew and Tarney, 1984; Jordan et al., 2001), or to strike-slip tectonics (Hervé et al., 1995). Submarine volcanism in the Traiguén Basin during the Cenozoic is significant because it indicates important crustal thinning (Mpodozis and Cornejo, 2012) and refutes the notion of a "Chilean subduction mode" in a permanent state of contraction as envisaged by Uyeda and Kanamori (1979). Also singular is the fact that the Traiguén Formation is the only known example of suprasubduction submarine volcanism in southern South America during the Cenozoic.

The present contribution investigates the tectono-sedimentary setting of the Traiguén Formation, integrating information from sedimentology, ichnology, petrography, geochemistry, structural geology, foraminiferal micropaleontology, and U-Pb geochronology. Based on our findings and previous geologic studies in this region, we delve into the causes of subsidence and submarine volcanism in the Traiguén Basin and explore the relation of this event to Cenozoic plate kinematics along the Chilean margin.

GEOLOGIC SETTING

The Traiguén Formation (~44°S–46°S) is located on the forearc and western flank of the North Patagonian Andes (Figs. 1 and 2). This segment of the Andean Cordillera extends between ~38°S and 47°S and presents significant differences when compared with the Central Andes to the north, including lower elevation (1–2 km) and width (~300 km), reduced crustal thickness (~40 km), and less shortening (12–25 km) (Mpodozis and Ramos, 1990; Hervé, 1994; Ramos and Ghiglione, 2008; Orts et al., 2012). Also distinctive of the North Patagonian Andes is an ~1000 km, trench-parallel, dextral strike-slip fault system referred to as the Liquiñe-Ofqui fault zone (Hervé 1994; Cembrano et al., 2002). An active spreading center, the Chile Rise, is currently subducting at ~46°S and defines the Chile triple junction between the Nazca, South American, and Antarctic plates (Cande and Leslie, 1986).

Three N-S–trending physiographic units characterize the Chilean margin between ~33°S and 44°S: the Coastal Cordillera, the Central Depression, and the Main Andean Cordillera. The Coastal Cordillera and the Central Depression are not well defined in the study area, where the latter gradually narrows to the south and disappears at ~46°S–47°S (Cembrano et al., 2002; Silva, 2003). The Chonos Islands, with elevations up to ~1000 m, are remnants of the Coastal Cordillera after the deep glacial incision of this range during the Pleistocene and subsequent flooding of the valleys as sea level rose in the Holocene. In this region, fjords and islands characterize the Central Depression.

The most extensive rocks in the study area are (1) Paleozoic–Triassic metamorphic rocks, which crop out on most of the Chonos Islands and also on the western flank of the Andes in the southern part of the study area (Hervé et al., 2003); (2) Jurassic, Cretaceous, Eocene, and Miocene plutonic rocks of the North Patagonian Batholith, which crop out along most of the North Patagonian Andes and on the eastern Chonos Islands (Pankhurst et al., 1999); and (3) Mesozoic and Cenozoic sedimentary and volcanic rocks, which crop out principally on the eastern flank of the Andes and the Precordillera (Suárez and De La Cruz., 2000; Ramos and Ghiglione, 2008). Less extensive are late Oligocene–early Miocene volcano-sedimentary rocks of the Traiguén Formation exposed in a N-S belt between the metamorphic basement and the North Patagonian Batholith (Espinoza and Fuenzalida, 1971; Bobenrieth et al., 1983; Hervé et al., 1995) and late Oligocene–Miocene marine rocks that occur in small outcrops across the forearc, the North Patagonian Andes, and the Precordillera (De Vries et al., 1984; Frassinetti and Covacevich, 1999; Encinas et al., 2014, and references therein).

Previous Studies on the Traiguén Formation

The Traiguén Formation is a marine volcano-sedimentary unit that crops out on the islands and part of the mainland area of the Aysén region of southern Chile between ~44°S and 46°S (Figs. 1 and 2; Espinoza and Fuenzalida, 1971; Bobenrieth et al., 1983; Hervé et al., 1995). This unit was defined by Espinoza and Fuenzalida (1971), who designated Traiguén Island as its type locality. Subsequently, Bobenrieth et al. (1983) included in the Traiguén Formation the volcano-sedimentary rocks that crop out in the northern part of the study area (Magdalena Island and neighboring localities), which Fuenzalida and Etchart (1975) had previously described as the Puyuhuapi Formation.

The Traiguén Formation consists of interbedded pillow basalts, tuffs, breccias, sandstones, and shales (Espinoza and Fuenzalida, 1971; Bobenrieth et al., 1983; Hervé et al., 1995). Rocks of this unit in the northern part of the study area are metamorphosed to greenschist and amphibolite grades (Hervé et al., 1995; Silva, 2003). Although the Traiguén Formation overlies schists of the Paleozoic–Triassic metamorphic basement at Magdalena Island (Bobenrieth et al., 1983; Hervé et al., 1995), its actual stratigraphic thickness has not been determined because its exposures are limited to small coastal outcrops among the lush vegetation that characterizes this area. The Traiguén Formation is intruded by numerous basic aphanitic and doleritic dikes and locally by plutonic bodies of gabbroic to granodioritic composition (Hervé et al., 1995).

The age of the Traiguén Formation has been a matter of debate. Stiefel (1970) tentatively assigned rocks belonging to this unit to the Triassic–Early Tertiary interval. Fuenzalida and Etchart (1975) considered it to be Early

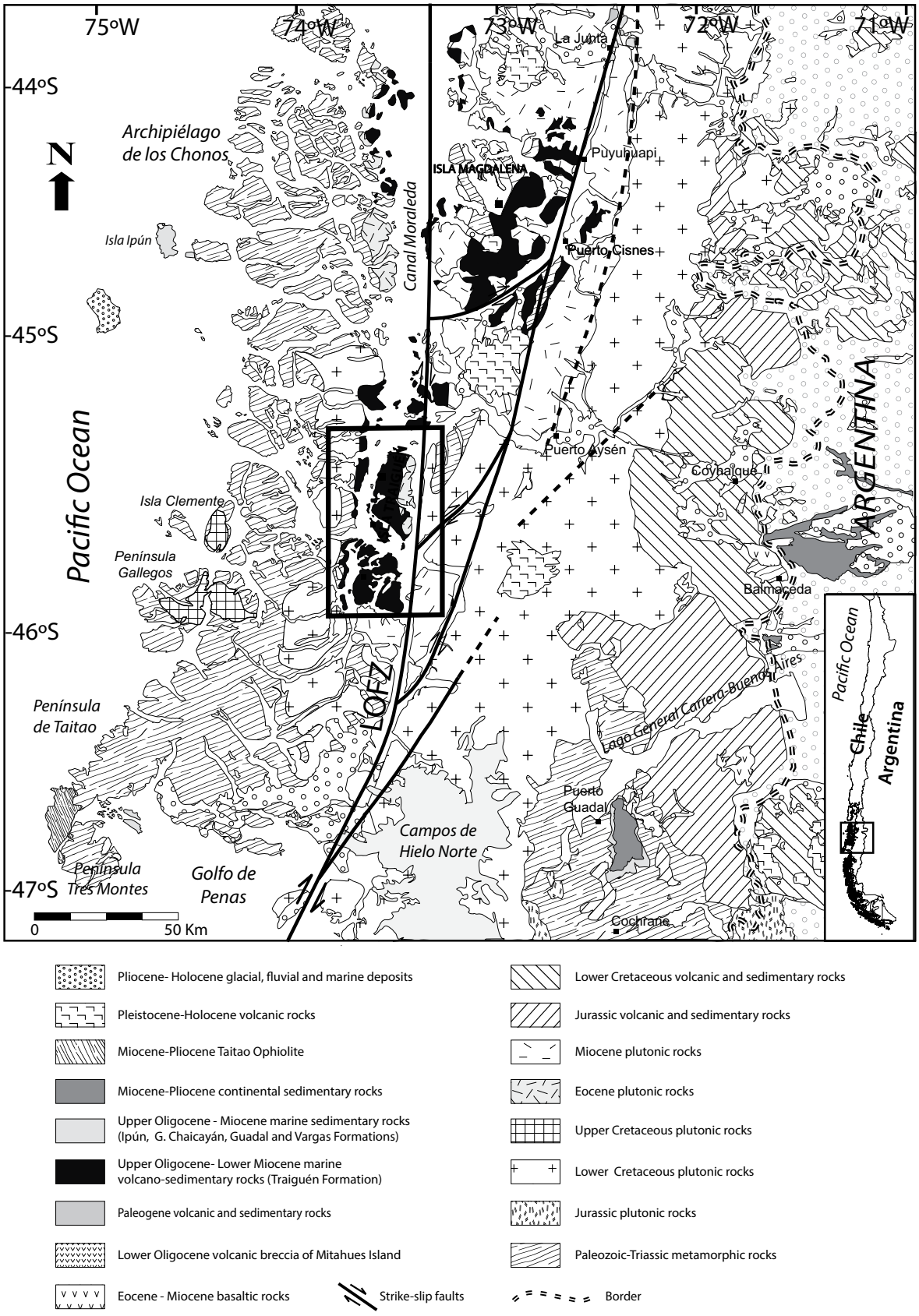

Figure 1. Regional geologic map. Inset is the area shown in Figure 2. Figure is after Segemar (1994, 1995); Pankhurst et al. (1999); Thomson (2002); Sernageomín (2003); Silva (2003). LOFZ—Liquiñe-Ofqui fault zone.

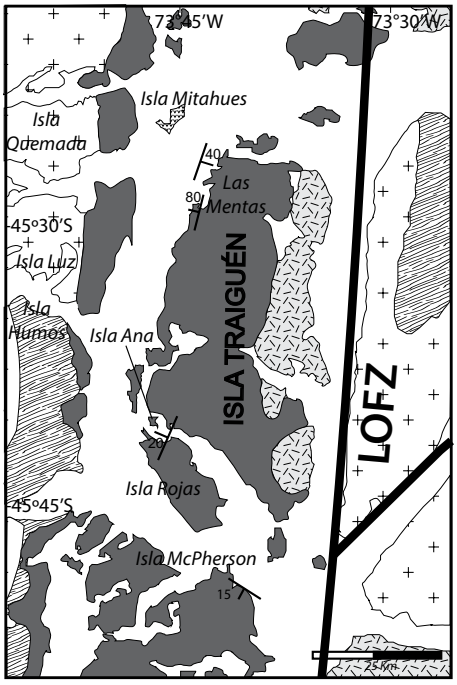

Figure 2. Map of study area showing geologic units and sample localities. See Figure 1 for key to the geologic units. LOFZ—Liquiñe-Ofqui fault zone.

Cretaceous based on the occurrence of poorly preserved marine fossils and on the erroneous assumption that it was intruded by Late Cretaceous plutonic rocks, which are now known to be Miocene in age (Pankhurst et al., 1999). Céspedes (1975) suggested a Miocene age for the Traiguén Formation based on planktonic foraminifera. Hervé et al. (1995) dated sedimentary and volcanic rocks of the Traiguén Formation at Magdalena Island with the Rb-Sr method and obtained two imprecise ages of 20 ± 28 Ma and 20 ± 26 Ma, but they noted that these most likely are the ages of metamorphism. Hervé et al. (2001) dated detrital zircons from a sandstone sampled from Traiguén Island and obtained a 26.0 ± 1.5 Ma U-Pb sensitive high-resolution ion microprobe (SHRIMP) maximum age for this unit. Silva et al. (2003) signaled, however, that the basal Traiguén Formation could be as old as Eocene based on the 38–15 Ma K/Ar ages obtained from a suite of dikes that they considered to be contemporaneous with the Traiguén Formation volcanic rocks.

SEDIMENTARY FACIES OF THE TRAIGUÉN FORMATION

Fieldwork was carried out on Traiguén Island and neighboring islands (Fig. 2). Due to the thick vegetation that characterizes the area, exposures of the Traiguén Formation are limited to short coastal cliffs. The basal and upper contacts of this unit at its type locality are not visible. The sedimentary rocks of the Traiguén Formation comprise interbeds of sandstone and siltstone, with minor conglomerate and breccia. They are locally interrupted by volcanic rocks, principally pillow basalts. We identified five sedimentary facies, as described next.

Rhythmically Interbedded Sandstone and Siltstone (T)

Description

This facies is composed of medium- to very coarse-grained sandstone rhythmically interbedded with siltstone (Fig. 3A). Beds are typically centimeters to decimeters thick, and they form partial Bouma cycles where sandstone predominates and is locally amalgamated. Sandstone typically shows Tb-c (parallel-convolute or, more rarely, ripple cross-lamination; Fig. 3B), Ta-b (massive-parallel), Tb (parallel), or Ta-c (massive-convolute) divisions. Sandstone bases are typically sharp, but load and flame structures occur at the contact with some siltstone beds, and some sandstone strata are crosscut by injection of the underlying siltstone (Fig. 3C). Fossils are generally absent from these facies, although some of the siltstones contain foraminifera and fragments of indeterminate macrofossils. Sandstone is primarily composed of quartz, plagioclase, and biotite.

Interpretation

The occurrence of rhythmically interbedded sandstone and siltstone forming Bouma cycles is characteristic of classic turbidites (Bouma, 1962; Posamentier and Walker, 2006). The common presence of convolute lamination, as well as the occurrence of load and flame structures and siltstone injections crosscutting the overlying beds, indicate rapid deposition of sediment that caused trapping of pore fluid and deformation of primary structures (Posamentier and Walker, 2006).

Massive Sandstone (Ms)

Description

This facies consists of medium- to coarse-grained massive (structureless) sandstone that may locally display zones of indistinct parallel lamination. Individual beds are up to a meter thick and locally form amalgamated stacks typically separated by thin partings of parallel-laminated sandstones. This facies is interbedded with classic turbidites (facies T), conglomerates (facies Cg), or siltstones and very fine sandstones (facies Sil). Basal contacts are commonly sharp and sometimes show load and flame structures and pseudonodules. Mineralogical composition of this facies is similar to that of sandstone in facies T.

Interpretation

Structureless sandstones are commonly interpreted as deposited by turbidity currents based on the common association of this facies with classic turbidites (Posamentier and Walker, 2006); however, other authors have postulated alternative depositional mechanisms, such as sandy debris flows (see Weimer and Slatt, 2007, and references therein). The presence of load and flame structures and pseudonodules indicates rapid deposition.

Siltstone and Very Fine-Grained Sandstone (Sls)

Description

This facies is composed of dark-gray siltstone and very fine-grained sandstone that locally form intervals a few meters thick and show relatively well-defined stratification, parallel lamination, and, more rarely, asymmetrical ripple marks. This facies is locally interbedded with classic turbidites (T) and conglomerates (Cg).

Interpretation

The small sizes of the outcrops in which we observed this facies prevent a refined interpretation, but the presence of interbedded turbidites indicates that it was probably deposited by distal turbidity currents and hemipelagic fallout.

Conglomerate (Cg)

Description

This facies consists of conglomerate beds that are typically decimeters thick and usually interbedded with turbidites, sandstones, siltstones, or lava flows. Basal contacts are sharp or erosive. The conglomerates are clast-supported and contain moderately to well-sorted, angular to subrounded clasts typically centimeters to decimeters in size. Its clasts are mostly pyroclastic lithics and more rarely andesite, basalt, or intraclasts of sandstone or siltstone. Typically, the conglomerate is normally graded with subtle stratification, and it often grades upward into tuffaceous sandstone.

Interpretation

Normal grading indicates transport by turbulent flows where grains moved freely relative to one another. Clast-supported conglomerates present in deep-marine successions are typically interpreted as having been deposited by turbidity currents (see Posamentier and Walker, 2006).

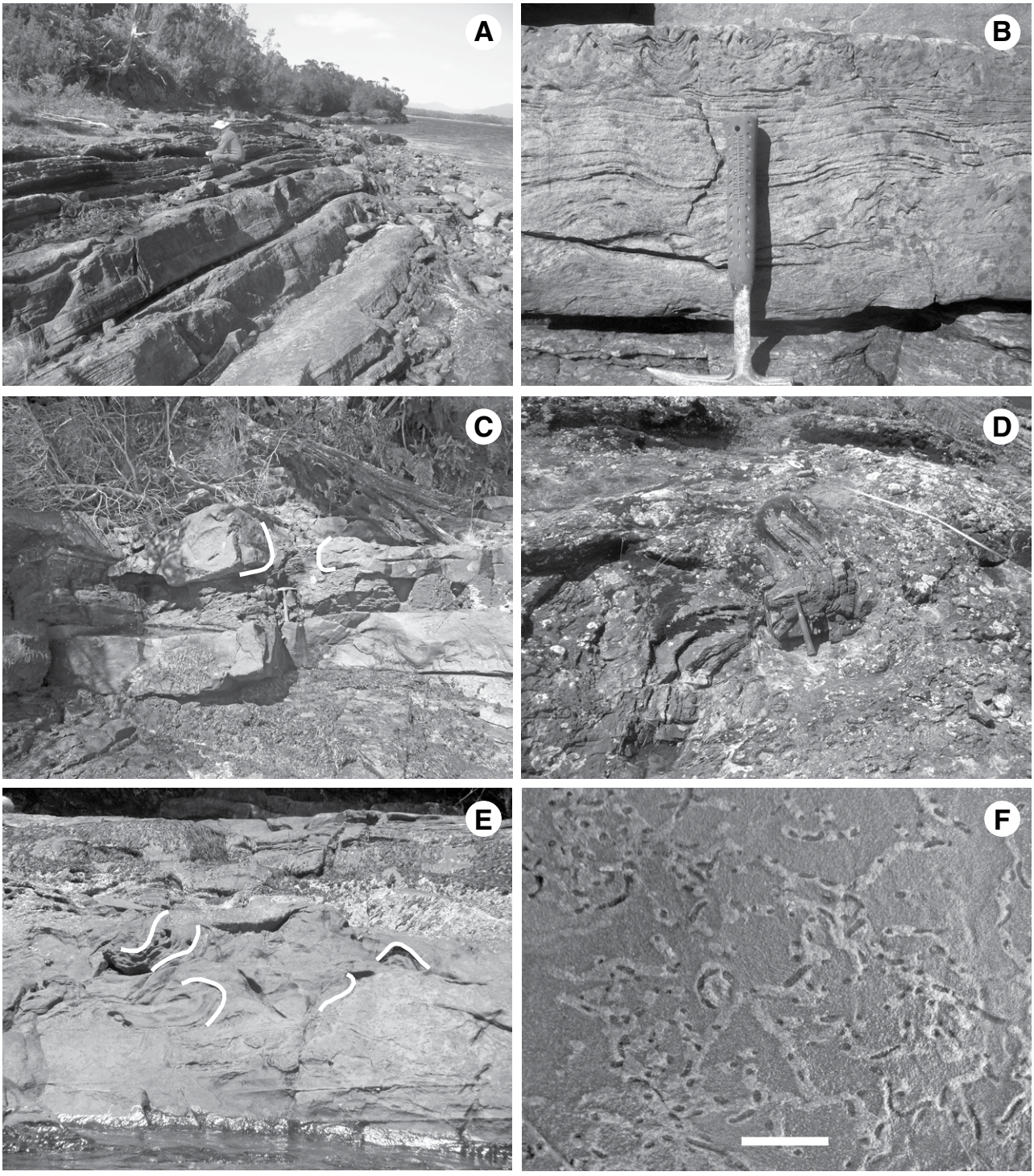

Figure 3. Characteristic facies and trace fossils of the sedimentary rocks of the Traiguén Formation. (A) Rhythmically interbedded sandstone and siltstone (facies T) at Las Mentas (Traiguén Island). (B) Detail of turbidite showing well-developed convolute lamination at the top. McPherson Island. (C) Turbidites showing sandstone strata crosscut by upward injection of the underlying siltstone. McPherson Island. (D) Intraformation breccia (facies Sl) with folded stratified block made of siltstone at Las Mentas (Traiguén Island). (E) Synsedimentary folded sandstone and siltstone. The fold's structure is partially delineated but difficult to follow due to intense deformation. McPherson Island. (F) *Phycosiphon incertum* in siltstone bed at Las Mentas (Traiguén Island). Scale is 1 cm.

The occurrence of rip-up clasts is evidence of turbulent scouring of the substrate immediately prior to deposition. The dominance of pyroclastic lithics in these facies suggests pyroclastic flows transformed into water-supported turbidity flows (see Cas and Wright, 1991).

Slumps (Sl)

Description

This facies is made up of chaotic, unbedded units that can be subdivided into intraformational breccia and synsedimentary folded strata. Intraformational breccia is massive, very poorly sorted, and several meters thick. Clasts are angular to subrounded, range in size from centimeters to several meters, are randomly oriented, and are typically siltstone, tuff, and more rarely basalt. Stratified blocks of siltstone, some of them folded (Fig. 3D), or interbedded pyroclastic breccia and tuff are common. Some of the large siltstone clasts contain benthic foraminifera indicative of bathyal depths. Synsedimentary folded sandstone and siltstone strata (Fig. 3E) form intervals a few meters thick that overlie and underlie flat-bedded successions.

Interpretation

As noted by Posamentier and Walker (2006), slumps consisting of intraformational breccias with stratified blocks were probably derived from collapse of submarine channel walls. Large blocks were probably rafted on top of mass-transport complexes that traveled short distances because the transport of stratified megaclasts in a turbulent medium or across long distances would probably result in their disintegration (Posamentier and Walker, 2006). The folded nature of some of the siltstone megaclasts indicates that they were unconsolidated, and the presence of bathyal foraminifera suggests that they were eroded from deposits of deep-water origin. Sandstone and siltstone strata with synsedimentary folding were formed by sliding of unconsolidated turbidites that were previously deposited in the basin and subsequently displaced downslope (Posamentier and Walker, 2006).

PETROGRAPHY AND GEOCHEMISTRY OF THE VOLCANIC ROCKS

Lava flows and related volcanic and subvolcanic rocks crop out in several localities along the coast of Traiguén and neighboring islands (Figs. 1 and 2). The lava flows are locally interbedded with sedimentary rocks (Fig. 4A) and exhibit features that are commonly associated with subaqueous volcanism, such as the pillows observed in outcrops on the Rojas, Traiguén, Ana, and Acuao Islands (Figs. 4A, 4B, 4C, and 4D). The pillows are well preserved, and the majority of them are <1 m in diameter. Some of them show a thin aphanitic rim that is slightly more altered than the rest of the pillow; these may be relicts of the glassy outer shell characteristic of water-magma interaction (Németh and Martin, 2007). The pillows also exhibit different types of surface features related to lava displacement or water-magma interaction (Németh and Martin, 2007), such as symmetrical spreading cracks (Fig. 4C), contraction cracks (Fig. 4D), and ropy wrinkles (Fig. 4B). Occasionally, flame structures occur in the contact between basaltic flows and sedimentary rocks, evidencing the load effect of the volcanic rocks on wet sediments. Massive, columnar-jointed flows lacking pillows occur locally. Hyaloclastites are rarer than lava flows and are characterized by fractured basalt fragments with curviplanar surfaces and a glass-rich matrix partially to completely replaced by palagonite that gives the rock its characteristic greenish-brown color. Pyroclastic breccias and tuffs, often of more intermediate composition than the effusive rocks, are locally interbedded with lavas and sedimentary rocks. Dikes and sills intrude the volcanic and sedimentary strata. Some of the dikes with pillow structures are connected to the lava flows, which indicates their contemporaneity.

Volcanic rocks assigned to the Traiguén Formation by Bobenrieth et al. (1983) also occur on the islands west and north of Traiguén Island, including Humos, Luz, and Mitahues (Fig. 2). The rocks at these localities include basaltic lavas and volcanic breccia with abundant basaltic dikes and sills. These volcanics are not interbedded with sedimentary rocks, nor do they show features indicative of subaqueous deposition. The U-Pb age of 32.2 Ma that we obtained for sample Isla Mitahues 1.1 (see following) suggests that they are older than the submarine lavas on Traiguén and its nearby islands.

The petrography of the Traiguén Formation lavas described here is detailed in Table DR1.[1] The rocks are porphyritic basalts with up to 20% phenocrysts of plagioclase, clinopyroxene, or mafic minerals completely altered to secondary phases and Fe-Ti oxides. The groundmass has an intersertal or intergranular texture with primary plagioclase and clinopyroxene and secondary devitrified glass. The original mafic phenocrysts most likely were olivine and clinopyroxene, with the latter more abundant. Phenocrysts exhibit skeletal textures and "swallowtails" attributed to water interaction and undercooling during the final stages of crystal growth after the emplacement of the lava flows (Lofgren et al., 1974).

All studied samples and most of the volcanic rocks of the Traiguén Formation are altered to some extent, but even though the alteration can be penetrative, their igneous textures and some original minerals are preserved. Pumpellyite and prehnite are the most abundant secondary mineral phases, as indicated by DRX (X-ray diffraction) analyses (Tapia, 2015); they occur mainly as the infilling of amygdules, in which they can be intergrown with calcite, quartz, or chlorite and form veinlets and aggregates replacing the original interpillow material. Plagioclase phenocrysts are partially replaced by sericite, clays, and minor chlorite. Seen in hand specimen, the milky luster of the feldspar phenocrysts suggests the Ca-Na exchange characteristic of the albitization processes of low-grade metamorphism (Frey and Robinson, 1999). Clinopyroxenes are completely to partially replaced by chlorite and minor quartz or calcite, whereas olivines are completely replaced by iddingsite and bowlingite. Plagioclase microliths in the groundmass are altered to sericite and clay, and the glass is devitrified to aggregates of chlorite/smectite, titanite, and Fe-oxyhydroxides. At the outcrop scale, the palagonitization process is inferred from the brownish green color of the devitrified matrix of hyaloclastites. However, palagonite is very difficult to recognize in petrographic sections, and it is thought to occur only within the groundmass, where it is almost indistinguishable from pure smectite aggregates.

Table DR2 lists the major- and trace-element contents in the studied samples along with the isotopic ratios of Sr, Nd, and Pb (see footnote 1). The analyzed rocks would plot in the basaltic-trachyandesite field of a classification diagram of Le Maitre (1989) based on their alkalis (N_2O, K_2O) and silica (SiO_2) contents. However, when plotted in diagrams based on the composition of more immobile elements (high field strength elements [HFSEs]), such as the Nb/Y versus Zr/Ti diagram for altered basalts (Winchester and Floyd, 1977), all of the samples plot in the area of subalkaline basalts. This agrees with the observed primary mineralogy devoid of an alkali-rich phase. The alkalis, Fe, and MgO contents of most samples correspond to the calc-alkaline series in the AFM (K_2O+N_2O-FeO*-Mg) classification of Irvine and Baragar (1971); only three samples plot over the line separating the calc-alkaline and tholeiitic fields. Since there is little variation on the SiO_2 content in the analyzed samples, most of the other elements do not reflect trends when compared to silica abundances; however, elements such as Ca, Mg, Al,

[1]GSA Data Repository item 2015373, petrography of volcanic and volcaniclastic rocks, elemental and isotopic composition of basalts, U-Pb LA-ICPMS zircon data, and foraminiferal data from the Traiguén Formation, is available at http://www.geosociety.org/pubs/ft2015.htm or by request to editing@geosociety.org.

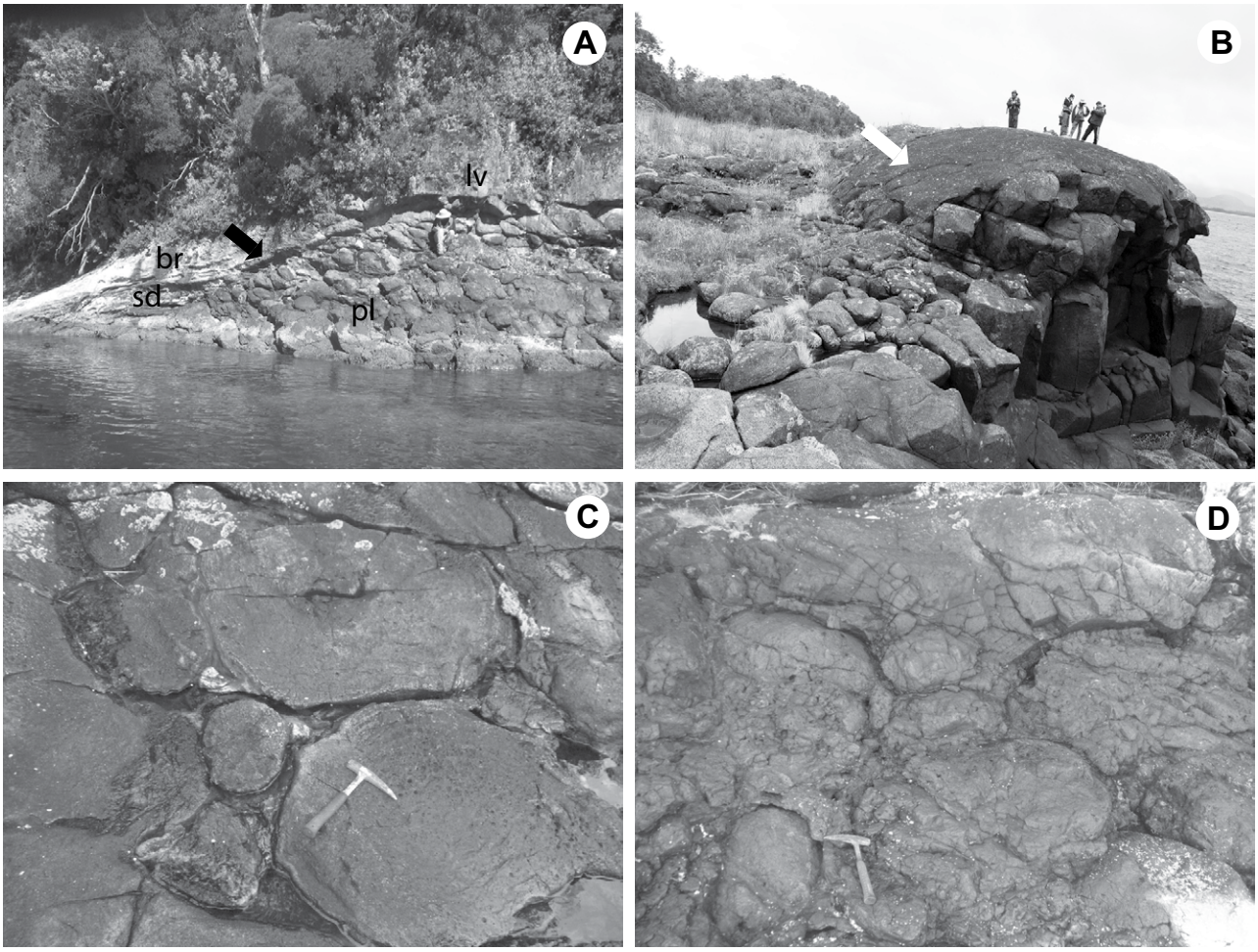

Figure 4. Volcanic rocks of the Traiguén Formation. (A) Sandstone (sd) and breccia (br) with basaltic clasts onlapping lava-flow deposits with well-developed pillows (pl). The three rocks are covered by a blocky lava flow (lv); Rojas Island. (B) Large lava flow (megapillow?) surrounded by pillows up to 1 m in size. The arrow on the left flank of the outcrop points to surface ridges interpreted as ropy wrinkles; Traiguén Island. (C) Cross section of several pillows showing light-colored rims interpreted as altered, quenched surfaces of the flow. Symmetrical spreading cracks are visible in the pillow outer part; Ana Island. (D) Contraction cracks around pillows; Acuao Island.

Ni, and Cr decrease with increasing Zr, whereas Na, K, P, Ti, Rb, Ba, Sr, Cu, rare earth elements (REEs), and HFSEs increase their abundance with increasing Zr. If Zr is taken as a differentiation indicator, the evolution of the volcanic rocks would have been controlled by fractional crystallization of olivine, clinopyroxene, and plagioclase.

The primitive mantle–normalized values for large ion lithophile elements (LILEs), HFSEs, and REEs show a pattern of decreasing content toward more compatible elements (Fig. 5A) along with a marked Nb-Ta negative anomaly (relative to LILEs). Chondrite-normalized REE values show low abundances, flat patterns, and no Eu anomalies (Fig. 5B), which are consistent with the less-differentiated character of the basalts. The isotopic composition of the studied rocks is rather homogeneous, with $^{87}Sr/^{86}Sr$ ranging 0.70467–0.705943, $^{143}Nd/^{144}Nd$ ranging 0.512904–0.512983, and $^{206}Pb/^{204}Pb$, $^{207}Pb/^{204}Pb$, and $^{208}Pb/^{204}Pb$ ranging 18.482–18.577, 15.586–15.626, and 38.343–38.468, respectively (Figs. 5C and 5D).

TRACE FOSSILS

Trace fossils in the sedimentary strata of the Traiguén Formation are scarce and generally show poor preservation. *Thalassinoides* isp. forms monospecific suites characterized by extensive horizontal networks at the top of some sandstone strata. *Taenidium*? isp. and *Scolicia* isp. are also present, but rare, in sandstone. *Phycosiphon incertum* (Fig. 3F) and *Chondrites* isp. occur in some siltstone beds.

Although the poor preservation of trace fossils precludes a refined interpretation, the association of *Phycosiphon incertum* and *Chondrites* isp. in the silty intervals is ascribed to the *Zoophycos* ichnofacies, which is characterized by low oxygen levels associated with high organic detritus in quiet-water settings, and which is typical of outer-shelf to slope settings (Frey and Pemberton, 1984). In the case of the Traiguén Formation, the *Zoophycos* ichnofacies characterizes interturbidite intervals of colonization. Monospecific suites of *Thalassinoides* isp. forming extensive horizontal networks characterize the *Skolithos* ichnofacies, which is typical of high-energy shallow-marine environments, but is also common in deep-water settings where it reflects local environmental conditions such as high energy, high levels of

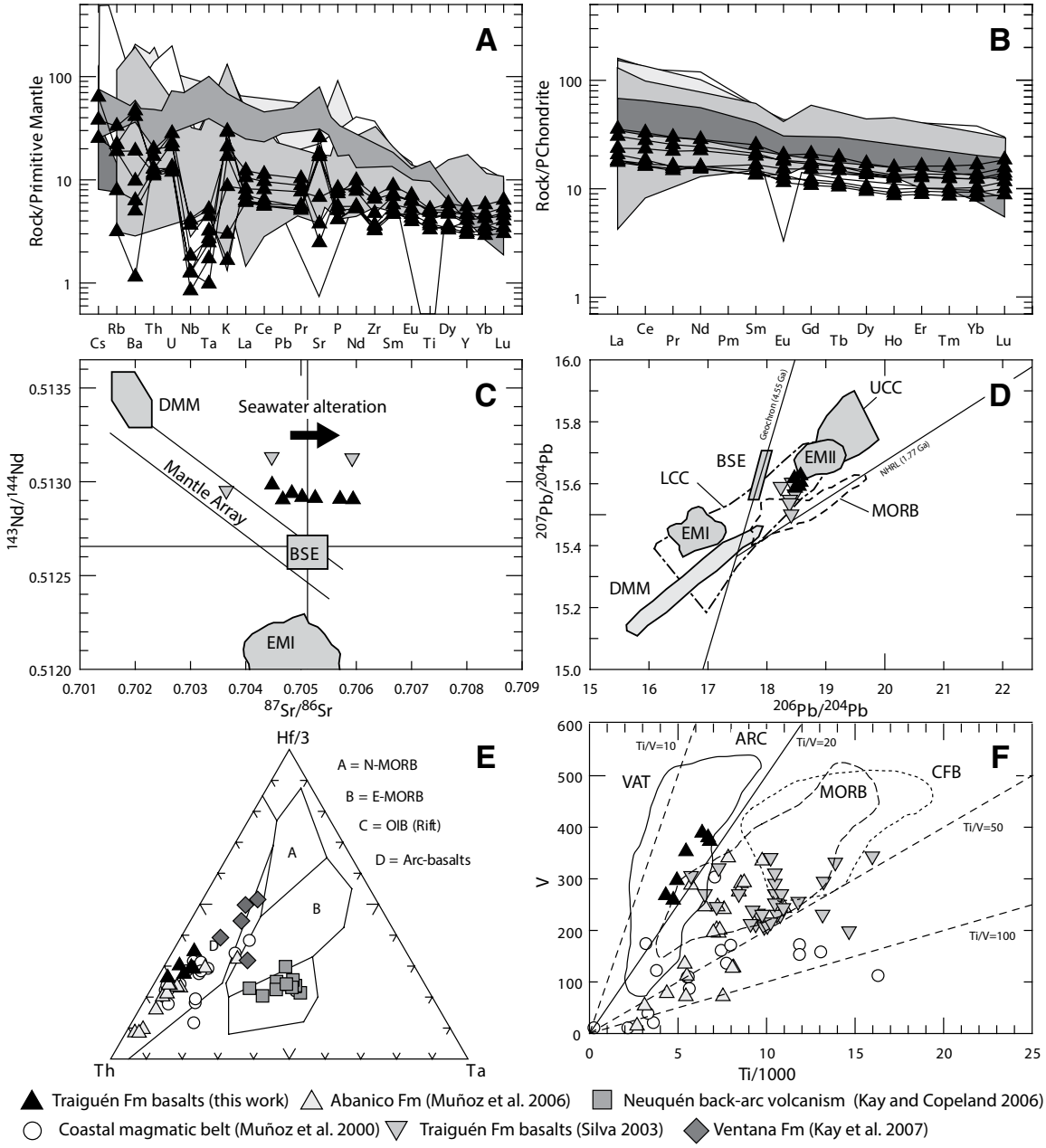

Figure 5. Geochemical plots of the studied rocks and other relevant volcanic units from central and south-central Chile and Argentina. (A) Primitive mantle–normalized contents of trace elements (normalizing values from Sun and McDonough, 1989). (B) Chondrite-normalized contents of rare earth elements (REEs; normalizing values from Sun and McDonough, 1989). (C) $^{143}Nd/^{144}Nd$ vs. $^{87}Sr/^{86}Sr$ diagram showing mantle domains (after Zinderl and Hart, 1986). (D) $^{207}Pb/^{204}Pb$ vs. $^{206}Pb/^{204}Pb$ diagram showing mantle domains (after Zinderl and Hart, 1986). (E) Tectonic discrimination diagram for basalts (Wood, 1980). (F) Tectonic discrimination diagram for basalts (Shervais, 1982). N-, E-MORB—normal, enriched mid-ocean ridge basalts; OIB—oceanic-island basalts; VAT—volcanic arc tholeiites; CFB—continental flood basalts; DMM—depleted mantle; BSE—bulk silicate earth; EMI-EMII—enriched mantle I and II; UCC-LCC—upper-lower continental crust; ARC—arc rocks. The rocks from the Coastal magmatic belt (Muñoz et al., 2000), the Abanico Formation (Muñoz et al., 2006), and the Magdalena Island basalts (Silva et al., 2003; this work) represent the arc domain (i.e., magmatism proximal to the plate margin). The rocks from the Neuquén Basin backarc volcanism (Kay and Copeland, 2006) and the Ventana Formation (Kay et al., 2007) represent the backarc domain (i.e., the domain distal to the plate margin).

oxygenation, sandy substrate, and an abundance of suspended organic particles (Buatois and López-Angriman, 1992). The *Skolithos* ichnofacies in the Traiguén Formation appears to be associated with the rapid deposition of sand.

FORAMINIFERA

A single rock sample was recovered by Céspedes (1975) from the northwestern part of Traiguén Island at Las Mentas (Fig. 2). The foraminifera in that sample (Sh-159) were studied by Mario Ernst (in Céspedes, 1975), who identified 23 benthic and two planktic species among the mostly poorly preserved specimens and concluded that the assemblage was Miocene and possibly bathyal (Tables DR3 and DR4 [see footnote 1]). Our revision of his foraminifera list indicates that about half of the benthic taxa have upper-depth limits on the slope. *Bathysiphon eocenicus* and *Melonis pompilioides* suggest that deposition may have been at lower bathyal (>2000 m) depths. Osorio (1989) reexamined this material and recorded eight benthic taxa identified only to genus, plus 16 planktic species. Osorio assigned an upper-lower to lower-middle Miocene age based on the concurrence of planktic species that had their first or last appearances in zone N8 (Tables DR3 and DR4 [see footnote 1]). He also interpreted the depth of the assemblage as upper bathyal because of its abundant planktic specimens and agglutinated benthic specimens, and the absence of miliolids.

According to current biostratigraphic data (BouDagher-Fadel, 2015), the Sh-159 planktic foraminiferal assemblage listed by Osorio (1989) indicates disparate ages. The concurrent range of most of the assemblage is early middle Miocene zone N11, which includes the first appearance of *Globigerina bulbosa* and the last appearance of *Globorotalia peripheroacuta*, but his assemblage includes *Globigerina binaiensis* and *Globigerina winkleri*, both of which have last appearance datums in early Miocene zone N5, and *Globigerina tripartite*, which has an Eocene–Oligocene range.

Our thin sections of seven rock samples were devoid of foraminifera. To isolate foraminifera for study, we processed seven siltstone samples from different stratigraphic sections of the Traiguén Formation in the study area, employing a variety of methods. Soaking in H_2O_2 and HCl failed to disaggregate the rocks, but immersion in 50% HF for 20 minutes succeeded in freeing some specimens. In addition, we chiselled out a few large specimens with a minimal amount of matrix from three rock samples. Our efforts enabled us to recognize only *Ammodiscus* sp. and *Bathysiphon* sp. (Fig. 6; Tables DR3 and DR4 [see footnote 1]). The specimens all show some degree of diagenetic alteration that mask potentially species-diagnostic features. These two benthic agglutinant genera, especially when represented by such large specimens, are most characteristic of upper-middle bathyal to lower-bathyal water depths but do not have biostratigraphic value in this study (Finger, 2013).

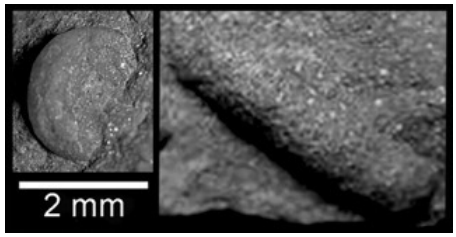

Figure 6. Large benthic agglutinated foraminifera in rock samples from Las Mentas (Traiguén Island). Left is *Ammodiscus* sp.; right is *Bathysiphon* sp.

U-Pb GEOCHRONOLOGY

Methodology

In order to determine the age of deposition and sedimentary provenance of the Traiguén Formation, we ran U-Pb analyses on 953 zircon grains extracted from one pyroclastic rock, one volcanic rock, and six sandstones (for location of samples, see Fig. 2). Heavy mineral concentrates of the <350 µm fraction from eight rock samples were separated using traditional techniques at ZirChron LLC (Tucson, Arizona). Zircons from the nonmagnetic fraction were mounted on a 1-in.-diameter (~2.5-cm-diameter) epoxy puck and then polished to expose the granular surface. After cathodoluminescence (CL) imaging at the University of Idaho, the laser ablation–inductively coupled plasma–mass spectrometry (LA-ICP-MS) U-Pb analyses were conducted at Washington State University (Pullman, Washington) using a New Wave Nd:YAG ultraviolet 213 nm laser coupled to a Thermo Scientific Element 2 single-collector, double-focusing, magnetic sector ICP-MS. Operating procedures and parameters are similar to those described in Chang et al. (2006). Laser spot size and repetition rate were 30 µm and 10 Hz, respectively. Each analysis consisted of a short blank analysis followed by 250 sweeps through masses 202, 204, 206, 207, 208, 232, 235, and 238, taking ~30 s. Time-independent fractionation was corrected by normalizing U/Pb and Pb/Pb ratios of the unknowns to the zircon standards (Chang et al., 2006). Concentrations of U and Th were monitored by comparison to NIST 610 trace-element glass standard. Two natural zircon standards were used: Plesovice, with an age of 337.13 ± 0.37 Ma (Sláma et al., 2008), and FC-1, with an age of 1099.0 ± 1.4 Ma (Paces and Miller, 1993). U-Pb ages were calculated and plots were generated using Isoplot (Ludwig, 2003; Fig. 7). The U-Pb zircon age errors for a set of analyses are reported using the quadratic sum of the analytical error plus the total systematic error (Valencia et al., 2005). Results are presented in Table DR5 (see footnote 1).

Results

Volcanic rock samples are characterized by clear pink euhedral zircon crystals, whereas sandstones included heterogeneous zircon populations presenting euhedral-subeuhedral to subrounded grains that ranged from clear pink to dark red-brown. CL images showed a great variation from single igneous-related oscillatory growth patterns to complex patterns. Almost all of the grains are characterized by Th/U ratios >0.1 (Table DR5 [see footnote 1]).

Zircons from sample Las Mentas 1.1 (lapilli tuff, Table DR6 [see footnote 1]) from Traiguén Island are dominantly late Oligocene and early Miocene. The calculated TuffZirc age (Ludwig, 2003) yielded a $^{206}Pb/^{238}U$ age of 23.4 ± 0.3Ma (n = 77, 2σ; Fig. 7). Older zircon ages of ca. 28 Ma are also present but in minor proportion.

A volcanic breccia (Table DR6 [see footnote 1]) was collected in the Mitahues Island (Isla Mitahues 1.1), and over 96% of the 122 zircon analyses yielded an early Oligocene age ($^{206}Pb/^{238}U$ TuffZirc age of 32.2 ± 0.4 Ma, 2σ; Fig. 7).

Detrital zircons from the Las Mentas 3.5 sandstone showed a major peak at ca. 23 Ma and smaller peaks in the Cretaceous, Paleozoic, and Precambrian (Fig. 7). The Las Mentas 12.1 sandstone was also characterized by a young peak (ca. 26 Ma maximum depositional age) and older peaks of 127, 280, and 1127 Ma (Fig. 7).

In contrast to the Las Mentas samples, the Isla Ana 1.1 sandstone lacked an early Miocene population (Fig. 7), although the sample included relatively similar Cretaceous to Precambrian peaks of 127, 287, 476, and 1085 Ma and older Mesoproterozoic and Paleoproterozoic zircon ages.

Sandstone samples from Isla Rojas (1.1 and 6.5) and McPherson 2.2 showed similar zircon populations as those in the other samples, although Isla Rojas 1.1 and McPherson 2.2 had rare late Oligocene 25–26 Ma age zircons (n = 2 and 1), and Isla Rojas 6.5 lacked the early Miocene detrital zircon component (Fig. 7).

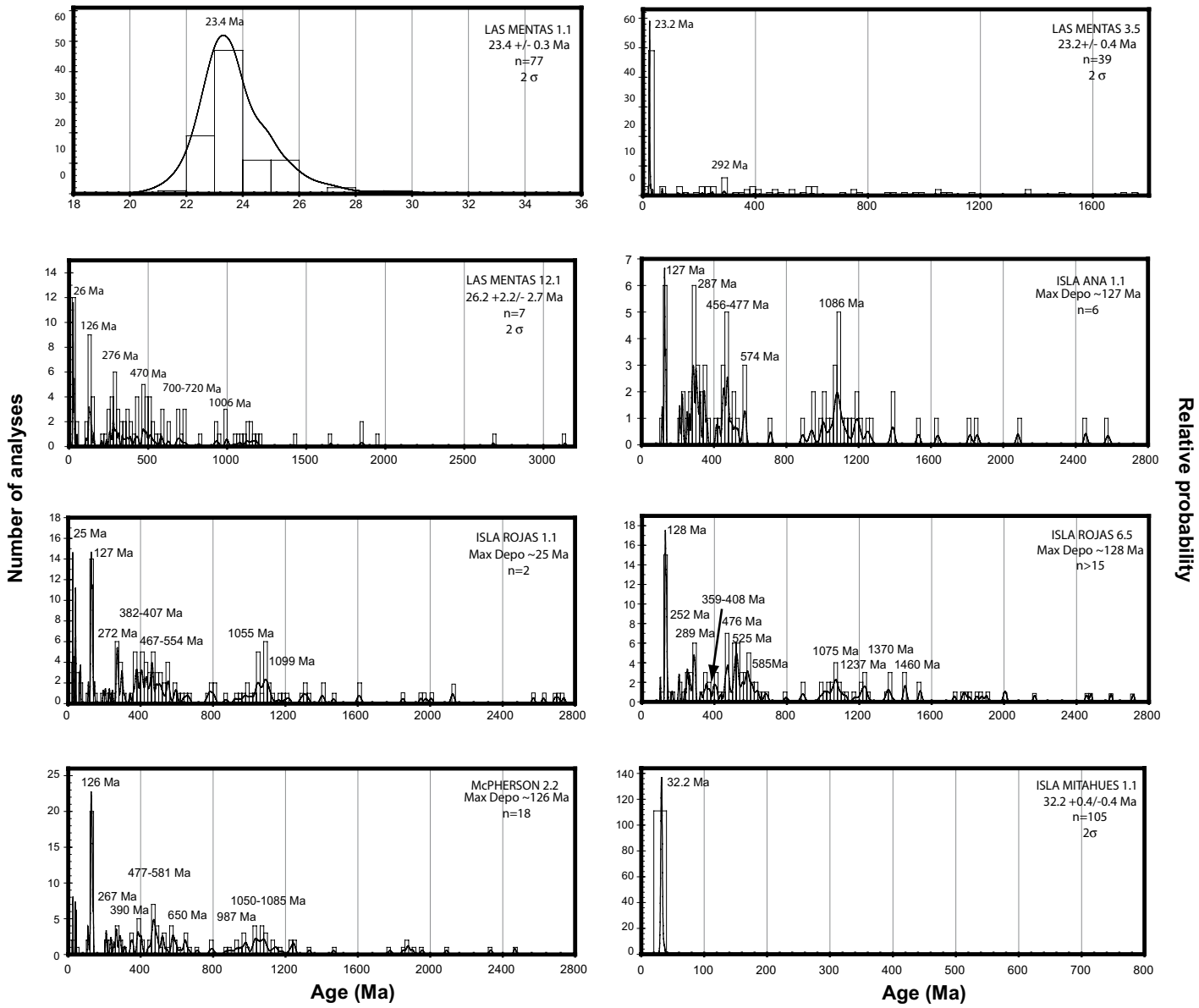

Figure 7. U-Pb ages and probability density plots for sandstones and tuffs from the Traiguén Formation and the Mitahues Island volcanic breccia.

EVIDENCE OF SYNEXTENSIONAL SEDIMENTATION

Extensional faults cut sedimentary and volcanic rocks of the Traiguén Formation in several outcrops of this unit. Normal faults are centimeters to meters long and at 70°–90° to the beds, which they offset up to 3 m (Fig. 8A). The listric geometry of some fault planes provokes the rotation of the hanging wall by a few degrees (Figs. 8A, 8C, and 8D). In general, normal faults show higher displacements in older strata than in younger strata, implying that fault movement was synchronous with sedimentation (Figs. 8C and 8D). In some cases, normal faults are associated with the injection of basaltic material (Fig. 8B). This observation implies that normal faults are related to crustal-tectonic processes and not merely to gravitational spreading.

DISCUSSION

Age of the Traiguén Formation

The youngest detrital zircon populations in four of the six sandstone samples from the Traiguén Formation yielded dates between ca. 23 and 26 Ma, indicating a late Oligocene–earliest Miocene maximum depositional age (Fig. 7). In addition, the lapilli tuff of sample Las Mentas 1.1 (Table DR6 [see footnote 1]), which was interbedded with sedimentary rocks in this unit, yielded an age of 23.4 ± 0.3 Ma. These new data agree with the ca. 26 Ma U-Pb SHRIMP maximum depositional age for a sandstone sample from the northwestern corner of the Traiguén Island reported by Hervé et al. (2001). Taken together, the consistency of these data may constrain the age of the Traiguén Formation to the late Oligocene–earliest Miocene; however, there is no complete section of this unit to confirm whether it spans a wider interval of time. A minimum age for the Traiguén Formation is probably constrained by the ca. 20 Ma age of

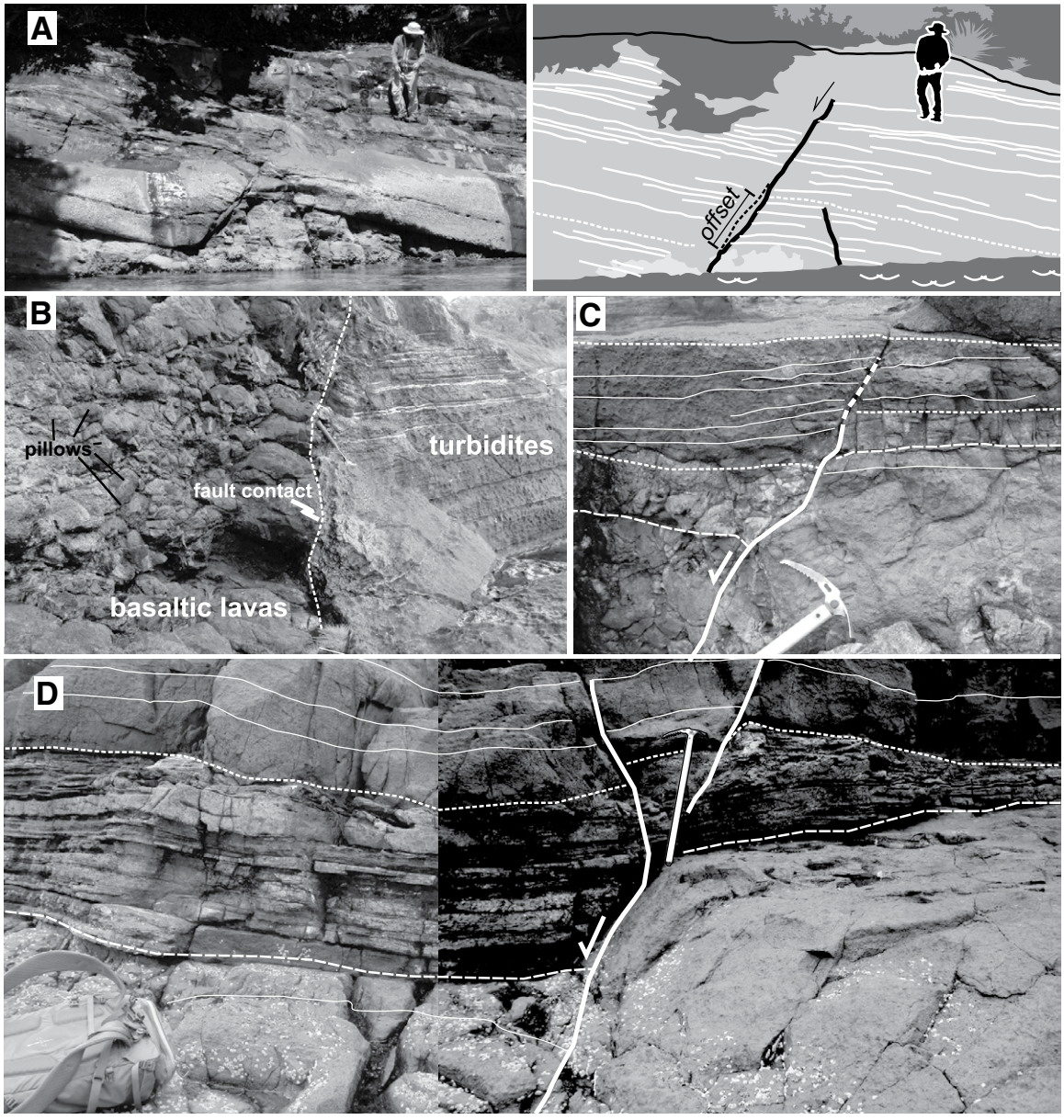

Figure 8. (A) Metric-scale normal faults in the Traiguén Formation strata on McPherson Island (see Fig. 2 for location). (B) Normal faults offsetting turbidites in the Traiguén Formation and associated with the injection of basaltic lava with pillow structures that indicate subsurface emplacement; on anonymous island close to northwestern Traiguén Island. (C–D) Metric-scale synextensional growth strata in turbidites of the Traiguén Formation on Rojas Island. Note that normal faults accommodate maximum thicknesses at the footwalls and that displacement is higher in the older strata and diminishes toward the top.

a pluton that intrudes the formation on Magdalena Island (Pankhurst et al., 1999; Hervé et al., 2001).

A review of previous age assignments for the Traiguén Formation that were obtained by other methods reveals some disagreements with our data. The Early Cretaceous age assigned to this unit by Fuenzalida and Etchart (1975) was principally based on the assumption that the plutonic rocks intruding the Traiguén Formation were Late Cretaceous, but subsequent studies revealed them to be Miocene (Pankhurst et al., 1999). Hervé et al. (1995) obtained two Rb-Sr ages of 20 ± 28 Ma and 20 ± 26 Ma from sedimentary and volcanic rocks on Magdalena Island, but they noted these ages most likely correspond to their metamorphism. Dikes cropping out in the Aysén region were dated by K/Ar at 38–15 Ma (Silva et al., 2003, and references therein) and considered to be contemporaneous with volcanism of the Traiguén Formation; some of these dikes do not intrude this unit and could be older, whereas those that crosscut the Traiguén Formation strata could be younger. Finally, the planktic foraminiferal assemblage of Traiguén Island sample Sh-159, assigned to the Miocene by Mario Ernst (in Céspedes, 1975), was restricted by Osorio (1989) to the lower–middle Miocene (Table DR4 [see footnote 1]). Their determinations must be taken

with caution, as both noted poor preservation. In addition, the species listed by Osorio (1989) indicate discordant biostratigraphic ranges.

The Traiguén Formation was originally defined by Espinoza and Fuenzalida (1971) on Traiguén Island. Bobenrieth et al. (1983) later augmented this unit with the volcano-sedimentary rocks of Magdalena Island and neighboring localities (Fig. 1). Yet, there are no reliable dates for the successions that crop out in the northern localities, as noted herein. Given the occurrence of pillow metabasalts assigned to the Paleozoic accretionary complex (Pankhurst et al., 1992) of the North Patagonian Andes at ~42°S, we cannot discard the possibility that the volcano-sedimentary succession of Magdalena Island predates that of Traiguén Island. However, Hervé et al. (1995) defended the hypothesis that these rocks are at least Tertiary based on the initial $^{87}Sr/^{86}Sr$ ratio of 0.7049 ± 0.0005 for the slate isochron, and they also noted the unconformable contact over the Paleozoic basement. Another uncertainty is the correlation of the Traiguén Formation with the volcanic rocks exposed west and north of Traiguén Island (e.g., islands of Humos, Luz, and Mitahues; Figs. 1 and 2). Unlike the Traiguén Formation, these rocks are not interbedded with sedimentary strata and lack features typical of subaqueous deposition. A U-Pb age of 32.2 Ma obtained from a volcanic breccia on Mitahues Island (Fig. 7) strongly supports the notion that they are unrelated to the Traiguén Formation. This date is also important because it is the only reported evidence of early Oligocene magmatism in the area.

In summary, U-Pb ages obtained in this study and that of Hervé et al. (2001) indicate that the volcano-sedimentary marine rocks of the Traiguén Formation at its type locality were deposited between ca. 23 and 26 Ma (late Oligocene–earliest Miocene). Whether the early Oligocene volcanic breccia of Mitahues Island forms part of the initial stage of volcanism in the Traiguén Basin or constitutes a different depositional sequence is uncertain. Also unclear is the correlation of the pillowed metabasalts of Magdalena Island and its neighboring area with the Traiguén Formation.

Tectono-Sedimentary Setting

The occurrence of syndepositional normal faults in the Traiguén Formation indicates that extension generated basin subsidence. The presence of well-preserved pillow lavas and hyaloclastites indicates that volcanism was subaqueous. The interbedded sedimentary rocks show facies characteristic of a deep-marine environment such as classic turbidites and slump deposits. Deep-marine deposition is further supported by the occurrence of the large benthic foraminifera of the typically bathyal genera *Ammodiscus* and *Bathysiphon* found in this study, as well as other taxa reported by Céspedes (1975) and Osorio (1989). The occurrence of the *Zoophycos* ichnofacies in fine-grained strata of this unit is also consistent with the sedimentologic data (Frey and Pemberton, 1984). All of the fossil evidence from the Traiguén Formation, however, must be taken with caution due to the poor preservation.

Analysis of provenance based on the age of detrital zircon populations from our samples (Fig. 7; Table DR5 [see footnote 1]) and the sample studied by Hervé et al. (2001) suggests that the Traiguén Formation sediment was derived from emerged areas located east and west of this unit (Fig. 1), which would support the idea that the outcrops of the Traiguén Formation correspond, at least approximately, with the original configuration of the basin. This inference, however, is uncertain because the geologic configuration of this region during deposition of the Traiguén Formation was subsequently modified by high exhumation rates that gave way to the erosion of most of the Mesozoic–Cenozoic volcano-sedimentary cover (Thomson, 2002; Adriasola et al., 2006) as well as the emplacement of the Miocene plutons of the Northern Patagonian Batholith (Pankhurst et al., 1999). The seven samples of the Traiguén Formation analyzed in this study yielded late Oligocene–early Miocene, Early Cretaceous, Triassic, Permian, Ordovician, Cambrian, and Proterozoic zircon ages. The youngest late Oligocene–early Miocene group likely derives from volcanism contemporaneous with deposition of the Traiguén Formation. Early Cretaceous zircons probably derive from plutonic rocks of the same age that extensively crop out east and west of the Traiguén Formation exposures. Triassic and older zircons were probably recycled from the metamorphic rocks widely exposed in the area, principally west of the Traiguén outcrops. A notable feature is the limited representation of Triassic zircons, which are abundant in the Chonos metamorphic complex (also noted by Hervé et al., 2001). Hervé et al. (2001) cited the presence of late Oligocene, Late Cretaceous, earliest Jurassic, Permian, and older Paleozoic and Proterozoic detrital zircon populations in their IT983 sample from the northwestern part of Traiguén Island. Noting an absence of Early Cretaceous zircons in their sample, they proposed that the plutonic rocks of this age, which presently crop out extensively in the area, were buried during deposition of the Traiguén Formation, but our results do not support that hypothesis. They also noted that the Late Cretaceous zircon population (which is absent in our samples) probably was derived from granitic rocks of the Peninsula Gallegos and Isla Clemente (Pankhurst et al., 1999), west of the Traiguén Basin (Fig. 1), as these are the only rocks of that age that crop out in the region.

According to their major-element contents, the basalts of the Traiguén Formation would have mostly a calc-alkaline affinity, but their abundant secondary mineral phases (e.g., pumpellyite, epidote, chlorite, prehnite, and white mica) could have significantly changed the FeO/MgO ratios, as well as the alkalis. In two samples (Mentas 3.1 and Ana 1.4), the K_2O and TiO_2 concentrations are particularly low. In all the analyzed basalts, the LILEs exhibit larger dispersion than the HSFEs, likely due to the hydrothermal alteration and/or low-grade metamorphism that affected the volcanic rocks; therefore, a reliable approach to clarifying magmatic sources or tectonic setting must be used on the basis of HFSE and REE abundances. Most of the Traiguén Formation basalts plot in the field of arc basalts or arc tholeiites, although two sample plots are close to the mid-ocean-ridge basalt (MORB) field (Figs. 5E and 5F), thus confirming the subduction-related nature of the volcanism. Isotopes of Sr and Nd suggest that the source of the Traiguén magma was a combination of a depleted mantle and a more-enriched component such as the continental crust (Fig. 5C). The interaction between magma and seawater is inferred from the decoupling between the isotopic systems, which is indicated by the marked shifting of $^{87}Sr/^{86}Sr$ ratios toward more radiogenic values. Radiogenic Sr likely was incorporated from seawater in the secondary mineral phases, whereas the magmatic isotope composition of insoluble Nd remained unchanged. Isotopes of Pb suggest the addition of sediments to the magmatic source, as the ^{207}Pb content is slightly higher than that of the MORB (Fig. 5D) source, requiring a crustal component mixed with a hypothetical depleted subarc mantle.

The geochemistry of the basalts in the Traiguén Formation is similar to other late Oligocene–early Miocene volcanic rocks of central and south-central Chile and Argentina, which have been interpreted as having been deposited in an extensional tectonic regime (e.g., Muñoz et al., 2000; Jordan et al., 2001; Kay and Copeland, 2006; Aragón et al., 2011, 2013; Litvak et al., 2014). However, the Traiguén volcanics show a more marked subduction signature. When compared to the contemporaneous volcanic units in the arc (closer to the plate margin) and backarc (farther east of the plate margin) domains, LILE and HFSE contents in the Traiguén basalts show trends similar to those rocks located near the plate margin (Figs. 5A and 5E), being more abundant in LILEs (with the

exception of two samples that have low K, Sr, and Ba) and significant negative Nb-Ta anomalies. The asthenospheric mantle, either depleted or oceanic-island basalt (OIB)-like, with little modification from a subducted slab, has been invoked as the main source for the majority of late Oligocene–early Miocene magmas (Muñoz et al., 2000; Silva, 2003; Kay and Copeland, 2006; Kay et al., 2007; Bruni et al., 2008; Aragón et al., 2013). However, it is not possible to attribute their origin solely to MORB- or OIB-like sources from the geochemistry of the studied samples (Figs. 5E and 5F), and the slab component is required to achieve their LILE compositions. Some authors have interpreted this as an inherited signal in the mantle source or the lithosphere from previous subduction processes (Muñoz et al., 2000; Aragón et al., 2013), possibilities that cannot be discarded for the Traiguén basalts. On the other hand, the Nd and Pb isotopic composition of the Traiguén basalts suggests a depleted to slightly enriched mantle source, which agrees with the models that propose a slab window (Aragón et al., 2011, 2013) or invigorated asthenospheric circulation in the mantle wedge (Muñoz et al., 2000).

The lack of a significant crustal contribution to the Traiguén Formation magmatism is also a feature shared with contemporaneous volcanic units, as evidenced by the isotopic composition and REE contents of the Traiguén basalts (Figs. 5B, 5C, and 5D). Furthermore, the Traiguén basalts plot in the island-arc or arc tholeiites domains in several discrimination diagrams, suggesting that the suprasubduction zone was located within a thinned crust and supporting the idea that a large portion of the Andean margin (~33°S–46°S) was under an extensional tectonic regime that stretched the continental crust (e.g., Muñoz et al., 2000; Jordan et al., 2001). The geochemical signature of the Tertiary? metabasalts from Magdalena Island, which Bobenrieth et al. (1983) included in the Traiguén Formation, suggest that they may have originated in a MORB-like tectonic environment (Hervé et al., 1995; Silva et al., 2003), a possibility that cannot be discarded for the Traiguén basalts. Yet, both sets of samples share similar characteristics, such as LILE enrichment over HFSE and Pb isotopic composition of an enriched mantle source (Figs. 5A, 5C, and 5D), which are often associated with subduction magmatism.

As indicated before, the secondary mineral phases present in the volcanic rocks (pumpellyite, prehnite, epidote, chlorite, calcite, quartz, iddingsite, fine-grained white mica, and titanite) and their occurrence as infillings of amygdules or veins, replacing phenocrysts or interpillow material, and in the groundmass are features that suggest very low-grade metamorphism in a submarine environment. A similar secondary mineralogy pattern has been also described by Silva (2003) for the basalts of Traiguén Island. We interpret this association as the prehnite-pumpellyite facies of low-grade metamorphism rather than the hydrothermal alteration observed in the mid-ocean-ridge seafloor, where smectite, celadonite, carbonates, zeolites, Fe-oxyhydroxides, and minor pyrite are the dominant phases due to the circulation of seawater heated by the magmatic system (Frey and Robinson, 1999). In fact, Oligocene–early Miocene volcanic rocks of the Abanico Formation show a similar prehnite-pumpellyite facies but were deposited under subaerial conditions (Muñoz et al., 2006). The basalts of the Traiguén Formation from the Magdalena Island area (Fig. 1), on the other hand, differ from those on Traiguen Island by having mineral assemblages that represent the greenschist, epidote-amphibolite, and amphibolite metamorphic facies. These were interpreted as diastathermal or contact metamorphism features by Hervé et al. (1993), but Hervé et al. (1995) and Silva (2003) later suggested the possibility that the metamorphism was an ocean-floor off-axis process.

Relation to Plate Convergence

Our data indicate that the deep-marine volcano-sedimentary rocks of the Traiguén Formation at its type locality were deposited in a suprasubduction extensional basin during the late Oligocene–early Miocene. Extension generated an attenuated crust that, according to conventional isostatic analyses, should have attained a thickness that did not exceed 33 km in order to allow the marine ingression (Introcaso et al., 2000). However, extension does not appear to have been sufficient to generate oceanic crust, as indicated by the geochemistry and metamorphic facies of the Traiguén basalts.

The causes of subsidence and subaqueous volcanism in the Traiguén Basin and its relation with plate convergence kinematics are debated. Bobenrieth et al. (1983) indicated that the Traiguén Formation formed in a forearc basin that had an oceanic volcanic arc and a marginal basin to the east, where the Cretaceous volcano-sedimentary Coyhaique Formation was deposited. That scenario was based in the erroneous assumption that the Traiguén Formation is Mesozoic. Hervé et al. (1995) suggested that the Traiguén Formation may have been deposited in pull-apart or asymmetric extensional basins (related to the dextral motion of the nearby strike-slip Liquiñe-Ofqui fault zone) as a consequence of oblique plate convergence between 45 and 25 Ma. To the contrary, our results indicate that the volcano-sedimentary rocks of the Traiguén Formation accumulated around 23–26 Ma, when convergence was more orthogonal (Pardo Casas and Molnar, 1987; Somoza, 1998). In addition, although the long-term nature, timing, and causes of lateral motion along the Liquiñe-Ofqui fault zone remain poorly understood, most data support the notions that this fault system formed after ca. 14 Ma and deformation is predominately transpressional (see Cembrano et al., 2002; Thomson, 2002; Encinas et al., 2013a).

Muñoz et al. (2000) and Jordan et al. (2001) described a regional episode of extensional tectonics that affected the Chilean margin between 33°S and 46°S during the late Oligocene–early Miocene. This event resulted in a series of extensional basins that extended from the present Chilean coast to the retroarc in Argentina and filled with thick successions of volcanic and sedimentary rocks. Correlation of the Traiguén Formation with the late Oligocene–early Miocene volcano-sedimentary deposits that crop out in such a large area indicates that subsidence and volcanism were likely caused by a more regional event than localized activity along the Liquiñe-Ofqui fault zone. Supporting this idea, Morata et al. (2005) and Bruni et al. (2008) obtained geochemical signatures suggestive of extensional tectonics from late Oligocene–early Miocene igneous rocks that crop out in the North Patagonian Andes and the retroarc at the same latitude as the Traiguén Basin. Also noteworthy is the occurrence of early Miocene (23–19 Ma) volcano-sedimentary deposits of the Ventana Formation in the North Patagonian Andes at 41°S–42°S, which consist of fossiliferous marine beds interbedded with basaltic rocks (Bechis et al., 2014), the latter of which show geochemical features indicative of a thinned crust (Bechis et al., 2014; Litvak et al., 2014).

The causes of extension and widespread volcanism during the late Oligocene–early Miocene in central and south-central Chile and Argentina are not well understood. Jordan et al. (2001) related this significant event in the history of the Chilean margin to the major plate reorganization in the southeast Pacific that resulted in a shift from slower, more oblique South America–Farallón convergence to more rapid, near-normal South America–Nazca convergence at ca. 26–28 Ma (see Pardo Casas and Molnar, 1987; Somoza, 1998). According to Jordan et al. (2001), this change gave way to a transient state of slab configuration and mantle circulation, which generated a wide zone of volcanic activity and extension, and this is inconsistent with models that link high convergence rates to strong mechanical coupling between the upper and lower plates (e.g., Pardo-Casas and Molnar, 1987). Alternatively, Muñoz et al. (2000) pro-

posed that the change in subduction geometry and the increase in trench-normal convergence rate during the late Oligocene induced a transient period of vigorous asthenospheric-wedge circulation, that triggered the slab rollback of the subducting Nazca plate that resulted in regional extension and widespread volcanism. Transient steepening of the subduction angle caused the westward expansion of the magmatic activity that gave way to the "mid-Tertiary Coastal magmatic belt" (Muñoz et al., 2000). After the middle Miocene, the subduction angle decreased, causing contractional deformation, inversion of the extensional basins, and the shift of magmatic activity to its current position in the Main Andean Cordillera (Muñoz et al., 2000). Similarly, Kay and Copeland (2006) ascribed extensional conditions during this period to near-normal Nazca–South America plate convergence and slab rollback, which they related to slow relative motion between South America and the underlying mantle. In contrast to previous hypotheses, Aragón et al. (2011, 2013) related synextensional volcanism in northern Patagonia to the collision of the Farallon-Aluk active ridge, which, according to these authors, evolved into a Farallon-Patagonia transform plate margin during the Paleogene to early Miocene subsequent to the detachment and sinking of the Aluk plate and the opening of a large slab window.

The aforementioned discrepancies indicate the necessity of further study to better understand the causes of regional extension and widespread volcanism during the late Oligocene–early Miocene. Nevertheless, we believe the model proposed by Muñoz et al. (2000) accounts for all the characteristic features of this interval because slab rollback, accelerated asthenospheric-wedge circulation, and steepening of the subduction angle can explain the generalized extension and crustal thinning, widespread volcanism with a mixture of slab signature and pristine mantle sources, and occurrence of igneous rocks in the coastal area (Fig. 9). Maximum amounts of extension and crustal thinning on the Chilean margin during the late Oligocene–early Miocene occurred in the Traiguén and Ventana basins, as indicated by the occurrence of submarine volcanism in those areas.

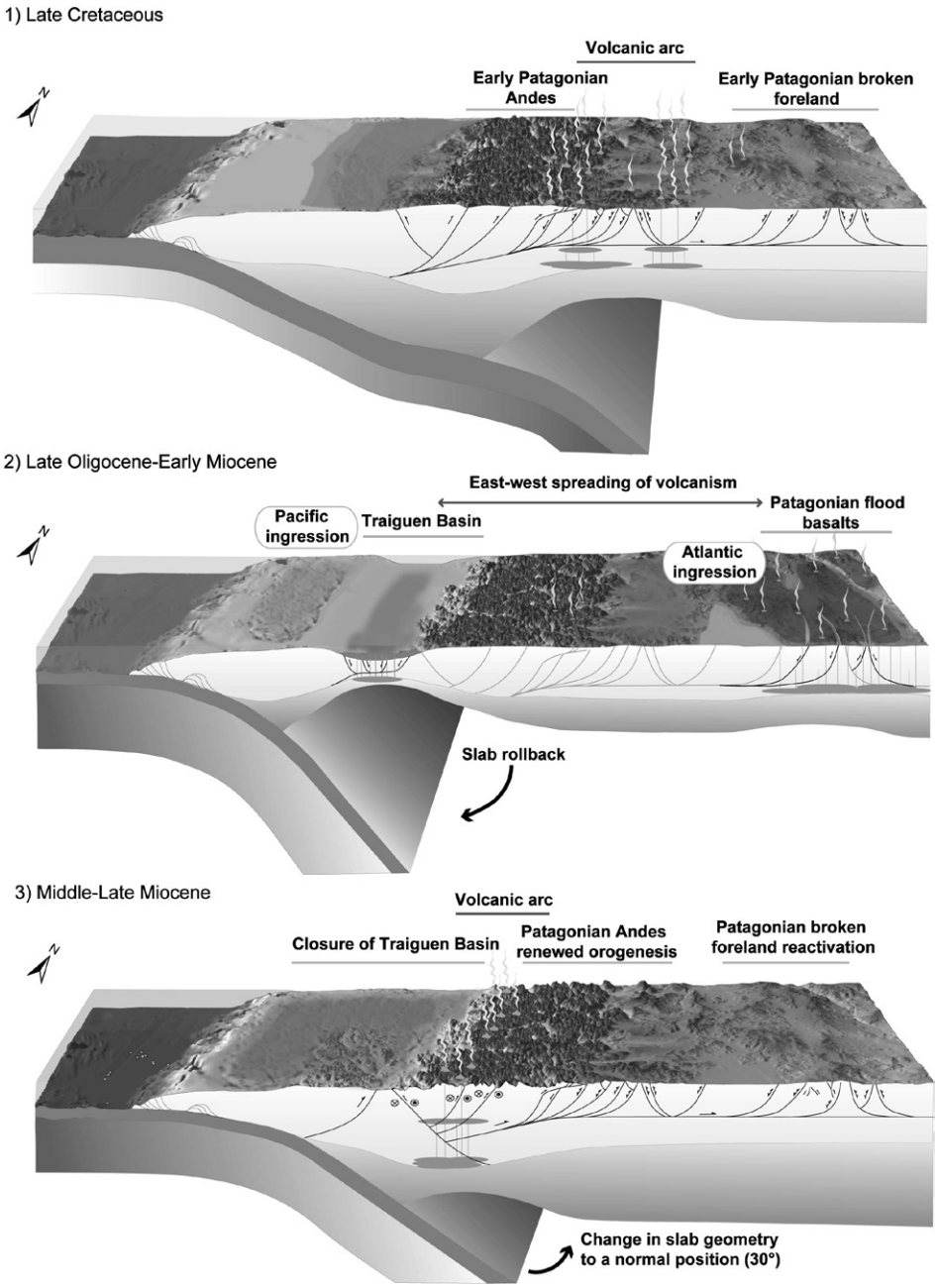

Figure 9. Cross sections showing the main tectonic phases that have impacted the study area since the late Mesozoic and the inferred changes in the slab geometry during the Oligocene–Miocene (based on model of Muñoz et al., 2000; see text for further explanation). (1) Late Cretaceous compression. (2) Late Oligocene–early Miocene extension, widespread volcanism, and Pacific and Atlantic marine transgressions triggered by slab rollback, intensified asthenospheric wedge circulation, and the steepening of the subduction angle. (3) Middle–late Miocene compression, inversion of the extensional basins, and the return of magmatic activity to its current position in the Main Andean Cordillera caused by the decrease of the subduction angle.

Implications for the Evolution of the North Patagonian Andes

The late Oligocene–early Miocene extensional regime that gave way to submarine volcanism in the Traiguén Basin represents a singular event in the development of the North Patagonian Andes. This mountain chain began developing during the late Early Cretaceous when major plate reorganization related to the breakup of southern Gondwana resulted in the tectonic inversion of the Jurassic–Early Cretaceous extensional basins (Mpodozis and Ramos, 1990; Suárez and De La Cruz, 2000; Folguera and Ramos, 2011). During the Paleocene–Eocene, the North Patagonian Andes experienced synextensional uplift, according to Aragón et al. (2011, 2013). Regional extension in this chain during the late Oligocene–early Miocene is evidenced by the onset of submarine volcanism in the Traiguén and Ventana basins,

the presence of synextensional strata observed in seismic profiles and outcrops (Jordan et al., 2001; Folguera et al., 2010; García Morabito and Ramos, 2012; Orts et al., 2012; Bechis et al., 2014) and the geochemistry of the volcanic rocks, which reflects a complex mixture of slab signature and pristine mantle sources (e.g., Muñoz et al., 2000; Jordan et al., 2001; Morata et al., 2005; Kay and Copeland, 2006; Bruni et al., 2008; Aragón et al., 2011; Litvak et al., 2014). An important phase of compressive and transpressive deformation and Andean uplift that commenced in the early–middle Miocene gave way to the inversion of the late Oligocene–early Miocene basins and to the present configuration of the North Patagonian Andes (Suárez and De La Cruz, 2000; Thomson, 2002; Adriasola et al., 2006; Blisniuk et al., 2005; Ramos and Ghiglione, 2008). Thus, the tectonic history of the North Patagonian Andes includes two notable phases of compression and uplift during the late Early Cretaceous and Neogene separated by moderate extension during the Paleocene–Eocene and maximum regional extension and subsidence in the late Oligocene–early Miocene (Fig. 9).

A debated issue concerning the tectonic and paleogeographic evolution of the North Patagonian Andes is the origin of the late Cenozoic marine deposits exposed in the forearc, Main Andean Cordillera, and retroarc of this region (e.g., Ramos, 1982; Frassinetti and Covacevich, 1999; Encinas et al., 2008; Bechis et al., 2014). Late Cenozoic marine deposits in the Chilean forearc crop out in several localities between ~33°S and 47°S (De Vries et al., 1984; Elgueta et al., 2000; Encinas et al., 2008, 2012). Coeval marine strata occur in small, disconnected outcrops in the western and eastern flanks of the North Patagonian Andes between ~40°S and 44°S at Lago Ranco, Ayacara, Río Foyel, and neighboring localities (Ramos, 1982; Orts et al., 2012; Encinas et al., 2013a, 2013b, 2014; Bechis et al., 2014; references therein). Late Cenozoic marine deposits of Atlantic origin, popularly known as the "Patagoniense," are exposed in several localities from the Atlantic coast of Argentina to the eastern flank of the North Patagonian Andes at Guadal, Chile (~47°S; Ramos, 1982; Frassinetti and Covacevich, 1999; Cuitiño et al., 2012).

The age and correlation of these marine deposits have been discussed for several years (Ramos, 1982; Frassinetti and Covacevich, 1999; Gutiérrez et al., 2012; Orts et al., 2012; Finger, 2013; Encinas et al., 2008, 2013a, 2013b, 2014; Bechis et al., 2014; references therein), but new data based principally on U-Pb geochronology favor a late Oligocene–early Miocene age (Orts et al., 2012; Cuitiño et al., 2012; Finger, 2013; Encinas et al., 2013a, 2013b, 2014; Bechis et al., 2014). Also debated is the possibility of an Atlantic–Pacific connection during deposition of these strata (e.g., Bertels, 1980; Ramos, 1982; Encinas et al., 2013a, 2014; Bechis et al., 2014). Recently, Encinas et al. (2014) reported the presence of both Pacific and Atlantic molluscan taxa in late Oligocene–early Miocene marine strata of the La Cascada and Vargas Formations (43°S–44°S), supporting the existence of a transient connection between the two oceans. The precise pathway of this connection, however, remains uncertain (see Bechis et al., 2014; Encinas et al., 2014; references therein).

The similar interpretations of a late Oligocene–early Miocene age for the described marine deposits and their widespread occurrence from the Pacific to the Atlantic coasts of Patagonia suggest that they reflect the same tectonic events. Most studies suggest that these strata were deposited under extensional regimes (Elgueta et al., 2000; Jordan et al., 2001; Giacosa et al., 2004; Melnick and Echtler, 2006), although some studies favor compressive deformation (Orts et al., 2012; Becerra et al., 2013). Bechis et al. (2014) proposed that the marine transgressions in the Río Foyel area (41°S–44°S) were related to the late Oligocene–early Miocene extensional tectonic stage proposed by Muñoz et al. (2000) and Jordan et al. (2001). They noted that the oldest marine strata in the region are ca. 23–19 Ma and interbedded with basaltic rocks of the Ventana Formation, evidencing the connection between subsidence and crustal thinning related to the extensional tectonics ascribed to deposition of this unit (Rapela et al., 1983; Kay and Copeland, 2006; Bechis et al., 2014; Litvak et al., 2014). Progressive extension caused general subsidence of the region that led to the marine incursion and deposition of the Río Foyel Formation and equivalent units (Bechis et al., 2014). The late Oligocene–earliest Miocene (26–23 Ma) volcano-sedimentary marine deposits of the Traiguén Formation appear to be coeval with most of the continental volcano-sedimentary deposits of south-central Chile and Argentina described by Muñoz et al. (2000) and Jordan et al. (2001), and slightly older than most of the late Cenozoic marine deposits of Patagonia (Azúa et al., 2012; Cuitiño et al., 2012; Orts et al., 2012; Encinas et al., 2013a, 2013b, 2014; Bechis et al., 2014). In agreement with the Bechis et al. (2014) model, we consider that the late Oligocene–early Miocene extensional event proposed by Muñoz et al. (2000) and Jordan et al. (2001) for the area between ~33°S and 46°S generated maximum extension in the Traiguén (46°S) and Ventana basins (41°S), as indicated by submarine volcanism in these areas. Progressive extension and crustal thinning resulted in marine flooding and the connection between the Pacific and the Atlantic oceans between ~41°S and 47°S. The subsequent phase of compressive tectonics that started around 16 Ma resulted in the emersion, uplift, and deformation of the late Oligocene–early Miocene marine strata concurrent with the growth of the North Patagonian Andes.

CONCLUSIONS

The results of our study indicate that the volcano-sedimentary Traiguén Formation was deposited in a deep-marine extensional basin during the late Oligocene–earliest Miocene. The geochemical and petrographic analyses suggest that the basalts of this unit represent the activity of subduction-related volcanism over a thinned crust. Although we cannot discard the role of the strike-slip Liquiñe-Ofqui fault system during the deposition of the Traiguén Formation, correlation of this unit with volcanic and sedimentary rocks deposited in extensional basins widely distributed in Chile and Argentina between ~33°S and 46°S indicates that the Traiguén Basin was likely formed as a consequence of a regional episode of extension and widespread volcanism during the late Oligocene–early Miocene. This event has been attributed to a transient period of slab rollback and intensified asthenospheric wedge circulation resulting from an increase in trench-normal convergence rate at ca. 26–28 Ma. Progressive extension and crustal thinning after the formation of the Traiguén Basin allowed a marine transgression of Pacific and Atlantic origin in Patagonia during the early Miocene. Compressive tectonics that began around 16 Ma resulted in the inversion of the Traiguén Basin concurrent with the uplift of the North Patagonian Andes. The Traiguén Formation constitutes the only reliable record of submarine suprasubduction volcanism during the Cenozoic in southern South America and our study of this unit confirms the importance of extensional tectonics along the Chilean margin during the late Oligocene–early Miocene.

ACKNOWLEDGMENTS

This research was funded by Fondecyt projects 1110914 and 1151146 of Conicyt. We appreciate the support provided by the Corporación Nacional Forestal of Chile (CONAF), the Consejo de Monumentos Nacionales de Chile (CMN), the Traiguén Island Huilliche community "Nahuelquín-Delgado," the assistance of the boat *Petrel* and its crew, and the help of Pablo Azúa during fieldwork. We are grateful to Nancy Riggs, Constantino Mpodozis, and Eugenio Aragón for their helpful suggestions and constructive comments, which considerably improved the manuscript.

REFERENCES CITED

Adriasola, A.C., Thomson, S.N., Brix, M.R., Hervé, F., and Stöckhert, B., 2006, Postmagmatic cooling and late Ce-

nozoic denudation of the North Patagonian Batholith in the Los Lagos region of Chile, 41°–42°15′S: International Journal of Earth Sciences, v. 95, p. 501–528.

Aragón, E., Castro, A., Díaz-Alvarado, J., and Liu, D.-Y., 2011, The North Patagonian Batholith at Paso Puyehue (Argentina–Chile). SHRIMP ages and compositional features: Journal of South American Earth Sciences, v. 32, no. 4, p. 547–554.

Aragón, E., Pinotti, L., D'Eramo, F., Castro, A., Rabbia, O., Coniglio, J., Demartis, M., Hernando, I., Cavarozzi, C.E., and Aguilera, Y.E., 2013, The Farallon-Aluk ridge collision with South America: Implications for the geochemical changes of slab window magmas from fore- to back-arc: Geoscience Frontiers, v. 4, p. 377–388.

Azúa, P., Encinas, A., Nielsen, S., and Valencia, V., 2012, Sedimentologic, ichnologic and paleontologic studies on the Neogene marine deposits of the Guafo, Ipún, Stokes and Lemo islands (43°30′–45°S, south-central Chile), *in* XIII Congreso Geológico Chileno: Antofagasta, Actas en Formato Digital, Simposio, v. 5, p. 701–702.

Bartholomew, D.S., and Tarney, J., 1984, Crustal extension in the southern Andes (45–46°S), *in* Kokelaar, B.P., Howells, M.F., and Roach, R.A., eds., Volcanic Processes in Marginal Basins: Geological Society of London Special Publication 16, p. 195–205.

Becerra, J., Contreras-Reyes, E., and Arriagada, C., 2013, Seismic structure and tectonics of the southern Arauco Basin, south-central Chile (~38°S): Tectonophysics, v. 592, p. 53–66.

Bechis, F., Encinas, A., Concheyro, A., Litvak, V.D., Aguirre-Urreta, B., and Ramos, V.A., 2014, New age constraints for the Cenozoic marine transgressions of northwestern Patagonia, Argentina (41°–43°S): Paleogeographic and tectonic implications: Journal of South American Earth Sciences, v. 52, p. 72–93.

Bertels, A., 1980, Foraminíferos (Protozoa) y ostrácodos (Arthropoda) de las "Lutitas de Río Foyel" (Oligoceno) de la cuenca de Ñirihuau, Provincia de Río Negro, República Argentina: Ameghiniana, v. 17, p. 49–52.

Blisniuk, P.M., Stern, L.A., Chamberlain, P.C., Idlemand, B., and Zeitlerd, P.K., 2005, Climatic and ecologic changes during Miocene surface uplift in the southern Patagonian Andes: Earth and Planetary Science Letters, v. 230, p. 125–142.

Bobenrieth, L., Díaz, F., Davidson, J., and Portigliati, C., 1983, Complemento Mapa Metalogénico XI Región, Sector Norte Continental, Comprendido entre 45° Latitud sur y el Límite con la X Región: Santiago, Chile, Sernageomín, 154 p.

BoughDager-Fadel, M.K., 2015, Biostratigraphic and Geological Significance of Planktonic Foraminifera, updated 2nd edition: London, UCL Press, 298 p.

Bouma, A.H., 1962, Sedimentology of Some Flysch Deposits: Amsterdam, Netherlands, Elsevier, 168 p.

Bruni, S., D'Orazio, M., Haller, M., Innocenti, F., Manetti, P., Pécskay, Z., and Tonarini, S., 2008, Time-evolution of magma sources in a continental back-arc setting: The Cenozoic basalts from Sierra de San Bernardo (Patagonia, Chubut, Argentina): Geological Magazine, v. 145, p. 714–732.

Buatois, L., and López-Angriman, A., 1992, The ichnology of a submarine braided channel complex: The Whisky Bay Formation, Cretaceous, James Ross Island, Antarctica: Palaeogeography, Palaeoclimatology, Palaeoecology, v. 94, p. 119–140.

Cande, S.C., and Leslie, R.B., 1986, Late Cenozoic tectonics of the southern Chile Trench: Journal of Geophysical Research, v. 91, p. 471–496.

Cas, R., and Wright, J.V., 1991, Subaqueous pyroclastic flows and ignimbrites: An assessment: Bulletin of Volcanology, v. 53, p. 357–380.

Cembrano, J., Lavenu, A., Reynolds, P., Arancibia, G., López, G., and Sanhueza, A., 2002, Late Cenozoic transpressional ductile deformation north of the Nazca–South America–Antarctica triple junction: Tectonophysics, v. 354, p. 289–314.

Céspedes, S., 1975, El Terciario de la Isla Traiguén y el Golfo de Tres Montes, Provincia de Aysén: Empresa Nacional del Petróleo (ENAP), Santiago, 5 p.

Chang, Z., Vervoort, J.D., McClelland, W.C., and Knaack, C., 2006, U-Pb dating of zircon by LA-ICP-MS: Geochemistry Geophysics Geosystems, v. 7, p. 1–14.

Charrier, R., Baeza, O., Elgueta, S., Flynn, J.J., Gans, P., Kay, S.M., Muñoz, N., Wyss, A.R., and Zurita, E., 2002, Evidence for Cenozoic extensional basin development and tectonic inversion south of the flat-slab segment, southern Central Andes, Chile (33°–36°S. L.): Journal of South American Earth Sciences, v. 15, p. 117–139.

Cuitiño, J.I., Pimentel, M.M., Ventura Santos, R., and Scasso, R.A., 2012, High resolution isotopic ages for the early Miocene "Patagoniense" transgression in southwest Patagonia: Stratigraphic implications: Journal of South American Earth Sciences, v. 38, p. 110–122.

De Vries, T., Stott, L., and Zinsmeister, W., 1984, Neogene fossiliferous deposits in southern Chile: Antarctic Journal of the United States, v. 29, no. 2, p. 12–13.

Dewey, J.F., and Bird, J.M., 1970, Mountain belts and the new global tectonics: Journal of Geophysical Research, v. 75, p. 2625–2647.

Encinas, A., Finger, K.L., Nielsen, S.N., Lavenu, A., Buatois, L.A., Peterson, D.E., and Le Roux, J.P., 2008, Rapid and major coastal subsidence during the late Miocene in south-central Chile: Journal of South American Earth Sciences, v. 25, p. 157–175.

Encinas, A., Finger, K.L., Buatois, L.A., and Peterson, D.E., 2012, Major forearc subsidence and deep-marine Miocene sedimentation in the present Coastal Cordillera and Longitudinal Depression of south-central Chile (38°30′S–41°45′S): Geological Society of America Bulletin, v. 124, no. 7–8, p. 1262–1277.

Encinas, A., Zambrano, P.A., Finger, K.L., Valencia, V., Buatois, L.A., and Duhart, P., 2013a, Implications of deep-marine Miocene deposits on the evolution of the North Patagonian Andes: The Journal of Geology, v. 121, p. 215–238.

Encinas, A., Zambrano, P., Bernabé, P., Finger, K., Buatois, L., Valencia, V., Fanning, M., and Hervé, F., 2013b, Tectonic implications of deep-marine Miocene strata in the western Andean Cordillera of south-central Chile (40°–42°S), *in* Rocha, R., et al., eds., 1st International Congress on Stratigraphy STRATI 2013: Lisboa, Simposio Regional Stratigraphy, Springer, p. 86.

Encinas, A., Pérez, F., Nielsen, S.N., Finger, K.L., Valencia, V., and Duhart, P., 2014, Geochronologic and paleontologic evidence for a Pacific-Atlantic connection during the late Oligocene–early Miocene in the Patagonian Andes (43–44°S): Journal of South American Earth Sciences, v. 55, p. 1–18.

Elgueta, S., McDonough, M., Le Roux, J., Urqueta, E., and Duhart, P., 2000, Estratigrafía y sedimentología de las cuencas terciarias de la región de Los Lagos (39–41°30′S): Boletín de la Subdirección Nacional de Geología, v. 57, p. 1–50.

Espinoza, W., and Fuenzalida, P., 1971, Geología de las Hojas Isla Rivero, Puerto Aysén y Balmaceda entre los Paralelos 45° y 46° de Latitud Sur: Santiago de Chile, Instituto de Investigaciones Geológicas Convenio Instituto CORFO Aysén, 50 p.

Finger, K.L., 2013, Miocene foraminifera from the south-central coast of Chile: Micropaleontology, v. 59, p. 341–493.

Folguera, A., and Ramos, V.A., 2011, Repeated eastward shifts of arc magmatism in the southern Andes: A revision to the long-term pattern of Andean uplift and magmatism: Journal of South American Earth Sciences, v. 32, p. 531–546.

Folguera, A., Rojas-Vera, E., Bottesi, G., Zamora-Valcarce, G., and Ramos, V.A., 2010, The Loncopué Trough: A Cenozoic basin produced by extension in the southern Central Andes: Journal of Geodynamics, v. 49, p. 287–295.

Frassinetti, D., and Covacevich, V., 1999, Invertebrados fósiles marinos de la Formación Guadal (Oligoceno Superior–Mioceno Inferior) en Pampa Castillo, Región de Aysén, Chile: Boletín del Servicio Nacional de Geología y Minería de Chile, v. 51, p. 1–96.

Frey, M., and Robinson, D., 1999, Low-Grade Metamorphism: Oxford, UK, Blackwell Publishing Ltd., 313 p., doi:10.1002/9781444313345.

Frey, R.W., and Pemberton, S., 1984, Trace fossils facies models, *in* Walker, R.G., ed., Facies Models: Geoscience Canada Reprint Series, p. 189–207.

Fuenzalida, R., and Etchart, H., 1975, Geología del Territorio de Aysén Comprendido entre los 43°45′ y los 45° Latitud Sur: Santiago, Chile, Instituto de Investigaciones Geológicas, 99 p.

García Morabito, E.G., and Ramos, V.A., 2012, Andean evolution of the Aluminé fold and thrust belt, Northern Patagonian Andes (38°30′–40°30′S): Journal of South American Earth Sciences, v. 38, p. 13–30.

Giacosa, R.E., Paredes, J.M., Nillni, A.M., Ledesma, M., and Colombo, F., 2004, Fallas normales de alto ángulo en el Neógeno del margen Atlántico de la Cuenca del Golfo San Jorge (46°S–67°30´O, Patagonia Argentina): Boletín Geológico y Minero, v. 115, no. 3, p. 537–550.

Gutiérrez, N., Hinojosa, L.F., Le Roux, J.P., and Pedroza, V., 2012, Evidence for an early–middle Miocene age of the Navidad Formation (central Chile): Paleontological, paleoclimatic and tectonic implications: Andean Geology, v. 40, p. 66–78.

Hervé, F., 1994, The southern Andes between 39° and 44°S latitude: The geological signature of a transpressive tectonic regime related to a magmatic arc, *in* Reutter, K.J., Scheuber, E., and Wigger, P., eds., Tectonics of the Southern Central Andes: Berlin, Springer-Verlag, p. 243–248.

Hervé, F., Suárez, M., and De la Cruz, R., 1993, Basic magmatism in a mid-Tertiary transtensional basin, Isla Magdalena, Aysén, Chile, *in* Second Symposium International Géodynamique Andine: Oxford, UK, ORSTOM, p. 367–369.

Hervé, F., Pankhurst, R.J., Drake, R., and Beck, M.E., 1995, Pillow metabasalts in a mid-Tertiary extensional basin adjacent to the Liquiñe-Ofqui fault zone: The Isla Magdalena area, Aysén, Chile: Journal of South American Earth Sciences, v. 8, no. 1, p. 33–46.

Hervé, F., Sanhueza, A., Silva, C., Pankhurst, R.J., Fanning, M.C., Campbell, H., and Crundwell, M., 2001, A Neogene age for Traiguén Formation, Aysén, Chile, as revealed by SHRIMP U-Pb dating of detrital zircons, *in* III Simposio Sudamericano de Geología Isotópica: Pucón, Chile, Servicio Nacional de Geología y Minería, p. 570–574.

Hervé, F., Fanning, C.M., and Pankhurst, R.J., 2003, Detrital zircon age patterns and provenance of the metamorphic complexes of southern Chile: Journal of South American Earth Sciences, v. 16, no. 1, p. 33–46.

Introcaso, A., Pacino, M.C., and Guspi, F., 2000, The Andes of Argentina and Chile: Crustal configuration, isostasy, shortening and tectonic features from gravity data: Temas de Geociencias, v. 5, 31 p.

Irvine, T.N., and Baragar, W.R.A., 1971, A guide to chemical classification of the common volcanic rock: Canadian Journal of Earth Sciences, v. 8, p. 523–548.

Jordan, T., Isacks, B.L., Allmendinger, R.W., Brewer, J.A., Ramos, V.A., and Ando, C.J., 1983, Andean tectonics related to geometry of subducted Nazca plate: Geological Society of America Bulletin, v. 94, p. 341–361.

Jordan, T., Matthew, W., Veiga, R., Pángaro, F., Copeland, P., Kelley, S., and Mpodozis, C., 2001, Extension and basin formation in the southern Andes caused by increased convergence rate: A mid-Cenozoic trigger for the Andes: Tectonics, v. 20, p. 308–324.

Kay, S.M., and Copeland, P., 2006, Early to middle Miocene backarc magmas of the Neuquén Basin: Geochemical consequences of slab shallowing and the westward drift of South America, *in* Kay, S.M., and Ramos, V.A., eds., Evolution of an Andean Margin: A Tectonic and Magmatic View from the Andes to the Neuquén Basin (35°–39°S Lat): Geological Society of America Special Paper 407, p. 185–213.

Kay, S.M., Ardolino, A.A., Gorring, M.L., and Ramos, V.A., 2007, The Patagonian Somuncura large igneous province: Interaction of a late Oligocene hotspot-like anomaly with a subducted slab: Journal of Petrology, v. 48, p. 43–77.

Lamb, S., and Davis, P., 2003, Cenozoic climate change as a possible cause for the rise of the Andes: Nature, v. 425, p. 792–797.

Le Maitre, R.W., 1989, A Classification of Igneous Rocks and Glossary of Terms: Recommendations of the IUGS Commission on the Systematics of Igneous Rocks: Oxford, UK, Blackwell, 158 p.

Litvak, V.D., Encinas, A., Oliveros, V., Bechis, F., Folguera, A., and Ramos, V.A., 2014, El volcanismo Mioceno inferior vinculado a las ingresiones marinas en los Andes Nordpatagónicos, *in* Martino, R.D., et al., eds., XIX Congreso Geológico Argentino: Córdoba, Argentina, ORSTOM, p. S22–S35.

Lofgren, G., Donaldson, C.H., Williams, R.J., Mullins, O., Jr., and Usselman, T.M, 1974, Experimentally reproduced textures and mineral chemistry of *Apollo 15* normative-quartz basalts: Geochimica and Cosmochimica Acta, v. 5, no. 1, supplement, p. 539.

Ludwig, K.R., 2003, Isoplot 3.0—A Geochronological Toolkit for Microsoft Excel: Berkeley Geochronology Center Special Publication 4, 71 p.

Martinod, J., Husson, L., Roperch, P., Guillaume, B., and Espurt, N., 2010, Horizontal subduction zones, convergence velocity and the building of the Andes: Earth and Planetary Science Letters, v. 299, p. 299–309.

Melnick, D., and Echtler, H.P., 2006, Inversion of forearc basins in south-central Chile caused by rapid glacial age trench fill: Geology, v. 34, p. 709–712.

Morata, D., Oliva, C., de la Cruz, R., and Suárez, M., 2005, The Bandurrias gabbro: Late Oligocene alkaline magmatism in the Patagonian Cordillera: Journal of South American Earth Sciences, v. 18, p. 147–162.

Mpodozis, C., and Cornejo, P., 2012, Cenozoic tectonics and porphyry copper systems of the Chilean Andes, *in* Hedenquist, J.W., Harris, M., and Camus, F., eds., Geology and Genesis of Major Copper Deposits and Districts of the World: A Tribute to Richard H. Sillitoe: Society of Economic Geologists Special Publication 16, p. 329–360.

Mpodozis, C., and Ramos, V., 1990, The Andes of Chile and Argentina, *in* Ericksen, G., Cañas, M., and Reinemund, J., eds., Geology of the Andes and its Relation to Hydrocarbon and Mineral Resources: Circum-Pacific Council for Energy and Mineral Resources, Earth Science Series, v. 11, p. 59–88.

Muñoz, J., Troncoso, R., Duhart, P., Crignola, P., Farmer, L., and Stern, C.R., 2000, The relation of the mid-Tertiary Coastal magmatic belt in south-central Chile to the late Oligocene increase in plate convergence rate: Revista Geológica de Chile, v. 27, p. 177–203.

Muñoz, M., Fuentes, F., Vergara, M., Aguirre, L., Nyström, J.O., Fèraud, G., and Demant, A., 2006, Abanico East Formation: Petrology and geochemistry of volcanic rocks behind the Cenozoic arc front in the Andean Cordillera, central Chile (33°50′): Revista Geológica de Chile, v. 33, no. 1, p. 109–140.

Németh, K., and Martin, U., 2007, Practical Volcanology: Lectures Notes for Understanding Volcanic Rocks from Field Based Studies: Geological Institute of Hungary Occasional Papers 207, 221 p.

Oncken, O., Hindle, D., Kley, J., Elger, K., Victor, P., and Schemmann, K., 2006, Deformation of the central Andean upper plate system—Facts, fiction, and constraints for plateau models, *in* Oncken, O., Franz, G., Giese, P., Götze, H.J., Ramos, V., Strecker, M., and Wigger, P., eds., The Andes—Active Subduction Orogeny: Berlin, Springer, Frontiers in Earth Sciences, p. 3–27.

Orts, D.L., Folguera, A., Encinas, A., Ramos, M., Tobal, J., and Ramos, V.A., 2012, Tectonic development of the North Patagonian Andes and their related Miocene foreland basin (41°30′–43°S): Tectonics, v. 31, p. TC3012, doi:10.1029/2011TC003084.

Osorio, R., 1989, Estudio Micropaleontológico de Material Sedimentario Proveniente de Bahía Mansa (Osorno); Isla Traiguén; Seno Hoppner (Península de Taitao) y Puerto Good (Isla Byron): Santiago, Chile, Empresa Nacional del Petróleo (ENAP), 12 p.

Paces, J., and Miller, J., 1993, Precise U-Pb ages of Duluth complex and related mafic intrusions, northeastern Minnesota; geochronological insights to physical, petrogenetic, paleomagnetic, and tectonomagmatic processes associated with the 1.1 Ga midcontinent rift system: Journal of Geophysical Research, v. 98, no. B8, p. 13,997–14,013, doi:10.1029/93JB01159.

Pankhurst, R.J., Hervé, F., Rojas, L., and Cembrano, J., 1992, Magmatism and tectonics in continental Chiloé, Chile (42°–42°30′S): Tectonophysics, v. 205, p. 283–294.

Pankhurst, R.J., Weaver, S., Hervé, F., and Larrondo, P., 1999, Mesozoic–Cenozoic evolution of the North Patagonian Batholith in Aysén, southern Chile: Journal of the Geological Society of London, v. 156, p. 673–694.

Pardo-Casas, F., and Molnar, P., 1987, Relative motion of the Nazca (Farallón) and South American plates since Late Cretaceous time: Tectonics, v. 6, no. 3, p. 233–248.

Posamentier, H.W., and Walker, R., 2006, Deep-water turbidites and submarine fans, *in* Posamentier, H.W., and Walker, R., eds., Facies Models Revisited: Society for Sedimentary Geology Special Publication 84, p. 399–520.

Ramos, V., 1982, Las ingresiones pacíficas del Terciario en el norte de la Patagonia (Argentina), *in* III Congreso Geológico Chileno (Actas): Concepción, Chile, Departamento de Geociencias, Universidad de Concepción, p. A262–A268.

Ramos, V.A., and Ghiglione, M.C., 2008, Tectonic evolution of the Patagonian Andes, *in* Rabassa, J., ed., Late Cenozoic of Patagonia and Tierra del Fuego: Developments in Quaternary Sciences 11: Ushuaia, Argentina, Elsevier, p. 57–71.

Rapela, C.W., Spalletti, L.A., and Merodio, J.C., 1983, Evolución magmática y geotectónica de la "Serie Andesítica" Andina (Paleoceno–Eoceno) en la Cordillera Norpatagónica: Revista de la Asociación Geológica Argentina, v. 38, no. 3–4, p. 469–484.

Russo, R., and Silver, P., 1996, Cordillera formation, mantle dynamics, and the Wilson cycle: Geology, v. 24, p. 511–514.

Segemar (Servicio Geológico Minero Argentino), 1994, Mapa Geológico de la Provincia de Río Negro: Republica Argentina Ministerio de Economía, Obras y Servicios Públicos, Buenos Aires, Argentina, scale 1:750,000.

Segemar (Servicio Geológico Minero Argentino), 1995, Mapa Geológico de la Provincia de Chubut: Republica Argentina Ministerio de Economía, Obras y Servicios Públicos, Buenos Aires, Argentina, scale 1:750,000.

Sernageomín (Servicio Nacional de Geología y Minería de Chile), 2003, Mapa Geológico de Chile, Versión Digital: Sernageomín Publicación Geológica Digital 4, CD-ROM, version 1.0, scale 1:1,000,000.

Shervais, J.W., 1982, Ti-V plots and the petrogenesis of modern and ophiolitic lavas: Earth and Planetary Science Letters, v. 59, p. 101–118.

Silva, C., 2003, Ambiente Geotectónico de Erupción y Metamorfismo de Metabasaltos Almohadillados de los Andes Norpatagónicos (42°–46°S), Chile [Tesis de magíster]: Santiago, Chile, Departamento de Geología, Universidad de Chile, 148 p.

Silva, C., Herrera, C., and Hervé, F., 2003, Petrogénesis de lavas y diques básicos de la Formación Traiguén, Región de Aysén (43°30′–46°S), Chile, *in* X Congreso Geológico Chileno: Concepción, Actas en CD-ROM, 11 p.

Silver, P.G., Russo, R.M., and Lithgow-Bertelloni, C., 1998, Coupling of South American and African plate motion and plate deformation: Science, v. 279, p. 60–63.

Sláma, J., Košler, J., Condon, D.J., Crowley, J.L., Gerdes, A., Hanchar, J.M., Horstwood, M.S.A., Morris, G.A., Nasdala, L., Norberg, N., Schaltegger, U., Schoene, B., Tubrett, M.N., and Whitehouse, M.J., 2008, Plešovice zircon—A new natural reference material for U-Pb and Hf isotopic microanalysis: Chemical Geology, v. 249, p. 1–35.

Somoza, R., 1998, Updated Nazca (Farallon)–South America relative motions during the last 40 My: Implications for mountains building in the central Andean region: Journal of South American Earth Sciences, v. 11, no. 3, p. 211–215.

Stiefel, J., 1970, El perfil de los Andes en la región del paralelo 45° Lat. Sur: Geologische Rundschau, v. 59, p. 961–979.

Suárez, M.R., and De La Cruz, R., 2000, Tectonics in the eastern central Patagonian Cordillera (45°30′S–47°30′S): Journal of the Geological Society of London, v. 157, p. 995–1001.

Sun, S.S., and McDonough, W.F., 1989, Chemical and isotopic systematics of oceanic basalts: Implications for mantle composition and processes, *in* Saunders, A.D., Norry, M.J., eds., Magmatism in the Ocean Basins: Geological Society of London Special Publication 42, p. 313–345.

Tapia, F., 2015, Edad y Condiciones de Depósito de las Rocas Volcánicas de la Formación Traiguén (45°25′–45°50′S) Aysén, Chile [Undergraduate Thesis]: Concepción, Chile, Universidad de Concepción, 85 p.

Thomson, S., 2002, Late Cenozoic geomorphic and tectonic evolution of the Patagonian Andes between latitudes 42°S and 46°S: An appraisal based on fission track results from the transpressional intra-arc Liquiñe-Ofqui fault zone: Geological Society of America Bulletin, v. 114, no. 9, p. 1159–1173.

Uyeda, S., and Kanamori, H., 1979, Back-arc opening and the mode of subduction: Journal of Geophysical Research, v. 84, p. 1049–1061.

Valencia, V.A., Ruiz, J., Barra, F., Geherls, G., Ducea, M., Titley, S.R., and Ochoa-Landin, L., 2005, U-Pb single zircon and Re-Os geochronology from La Caridad porphyry copper deposit: Insights for the duration of magmatism and mineralization in the Nacozari District, Sonora, Mexico: Mineralium Deposita, v. 40, no. 2, p. 175–191.

Weimer, P., and Slatt, R.M., 2007, Introduction to the Petroleum Geology of Deepwater Settings: American Association of Petroleum Geologists, Studies in Geology 57 (CD book), 816 p.

Winchester, J.A., and Floyd, P.A., 1977, Geochemical discrimination of different magma series and their differentiation products using immobile elements: Chemical Geology, v. 20, p. 325–343.

Wood, D.A., 1980, The application of a Th-Hf-Ta diagram to problems of tectonomagmatic classification and to establishing the nature of crustal contamination of basaltic lavas of the British Tertiary volcanic province: Earth and Planetary Science Letters, v. 50, p. 11–30.

Yañez, G., and Cembrano, J., 2004, Role of viscous plate coupling in the Late Tertiary Andean tectonics: Journal of Geophysical Research, v. 109, p. B02407, doi: 10.1029/2003JB002494.

Zindler, A., and Hart, S., 1986, Chemical Geodynamics: Annual Review of Earth and Planetary Sciences, v. 14, p. 493–571, doi:10.1146/annurev.ea.14.050186.002425.

Science Editor: David Ian Schofield
Associate Editor: Nancy Riggs

Manuscript Received 14 February 2015
Revised Manuscript Received 29 September 2015
Manuscript Accepted 9 November 2015

Printed in the USA